

EXPLORATION FOR BUILDING NEXT-GENERATION FOUNDATION MLLMs VIA SELF-LEARNING

000
001
002
003
004
005
006
007
008
009
010
011
012
013
014
015
016
017
018
019
020
021
022
023
024
025
026
027
028
029
030
031
032
033
034
035
036
037
038
039
040
041
042
043
044
045
046
047
048
049
050
051
052
053
Anonymous authors

Paper under double-blind review

ABSTRACT

While inference-time computation and post-training optimization have significantly advanced multimodal large language models (MLLMs), these advancements remain constrained by the capabilities of foundation models. We argue that effective model advancement requires strong synergy among pre-training, inference-time computation, and post-training optimization. In this paper, we introduce **Self-Improving cognition (SICOG)**, a self-learning framework for building next-generation foundation MLLMs by imparting multimodal knowledge and enhancing systematic cognitive capabilities through multimodal pre-training with self-generated data. Specifically, we propose *Chain-of-Description* for step-by-step visual understanding and integrate structured Chain-of-Thought (CoT) reasoning to support in-depth multimodal reasoning. SICOG first equips a base model with systematic perception and reasoning using minimal external supervision. The enhanced models then generate candidate image captions and CoT reasoning responses for *unlabeled* images and image-question pairs across diverse tasks, which are filtered through a semantic-similarity-guided self-consistency mechanism. These high-quality, self-generated samples enable large-scale multimodal pre-training, creating a self-improvement loop. Experiments demonstrate SICOG’s effectiveness in developing MLLMs with enhanced multimodal cognition. Using only 213K self-generated pre-training samples, SICOG achieves significant improvements, including +3.6% on MMStar and +3.5% on AI2D, outperforming previous pre-training approaches. When combined with post-training techniques for CoT reasoning, SICOG yields +9% gains on MMVet and +8.5% on ScienceQA.

1 INTRODUCTION

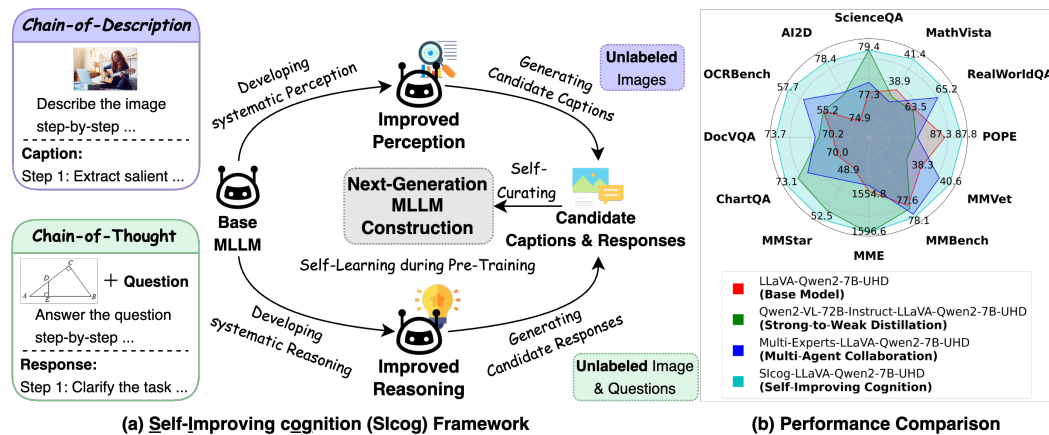


Figure 1: (a) SICOG enhances an MLLM’s systematic cognition during multimodal pre-training using self-generated data, enabling next-generation foundation MLLMs. (b) With up to 213K self-generated pre-training samples, SICOG produces foundation MLLMs with superior cognitive capabilities, showing benchmark-leading performance compared to prevalent pre-training approaches.

Recent efforts in inference-time computation (Teng et al., 2025) and post-training optimization (Guo et al., 2025; Feng et al., 2025) have significantly enhanced the capabilities of MLLMs (Yang et al., 2024b; Bai et al., 2023), particularly in areas such as multimodal reasoning (Xu et al., 2025). However, these advancements remain largely constrained by the foundational knowledge and capabilities of the models (Shah, 2024; Liu et al., 2025; Gandhi et al., 2025), which are determined during pre-training (Sutskever, 2024). **We argue that effective model advancement requires a strong synergy between pre-training and downstream mechanisms, such as inference-time computation and post-training optimization.** Pre-training provides the essential foundation, and its seamless integration with downstream processes is crucial for achieving robust and scalable performance.

In this paper, we focus on the effective advancement of foundation MLLMs (Li et al., 2024a), a critical step toward enabling real-world understanding (Bordes et al., 2024). Prevalent multimodal pre-training approaches for foundation MLLM construction (Chen et al., 2024a; Fang et al., 2024) typically rely on large-scale training with high-quality image–caption data generated by advanced MLLMs (OpenAI, 2023; Liu et al., 2024b) to equip models with diverse multimodal knowledge and fine-grained visual perception skills (Deng et al., 2024; Sun et al., 2024). Nonetheless, these generated captions often lack comprehensiveness and accuracy. To improve coverage, some methods incorporate fine-grained attributes using annotations from multiple expert models (Sun et al., 2024; Fang et al., 2024). However, the resulting captions often lack fluency and coherence due to the absence of an underlying logical structure. Moreover, these pre-training approaches tend to neglect the development of multimodal reasoning capabilities (Xu et al., 2025), which are essential for extending the practical utility of MLLMs in real-world applications (Li et al., 2024b).

Inspired by human experiential learning (*a.k.a.* human cognitive development) (Khatun et al., 2023; Silver & Sutton, 2025), we introduce **SICOG**, a self-learning framework that imparts multimodal knowledge and enhances MLLMs’ systematic cognitive abilities—including both perception and reasoning—during multimodal pre-training with self-generated data for next-generation foundation MLLM construction. Central to SICOG is *Chain-of-Description* (CoD), which enables an MLLM to interpret visual content through structured, step-by-step analysis. CoD sequentially focuses on four critical aspects—*salient content, fine-grained details, relational attributes, and peripheral context*—before generating a coherent and logically grounded description. This design ensures comprehensive coverage while mitigating hallucinations. We further incorporate structured CoT reasoning (Xu et al., 2025), which has been shown to significantly enhance complex reasoning by enabling in-depth multimodal analysis prior to answer generation and fostering coherent integration of visual and textual information. As illustrated in Figure 1 (left), SICOG first develops an MLLM’s systematic perceptual and reasoning capabilities using minimal external supervision. This is achieved by fine-tuning a base model on a small set of high-quality caption data enriched with our proposed *Chain-of-Description*, along with a limited amount of structured CoT reasoning data (**post-training optimization**). The fine-tuned model then generates multiple candidate captions and responses for *unlabeled multimodal data across diverse tasks*. To avoid dependence on external models, we apply a self-consistency mechanism (Wang et al., 2022; Wu et al., 2024) to curate these self-generated outputs, selecting higher-quality samples based on semantic coherence (**inference-time computation**). Finally, the curated data are used for large-scale multimodal **pre-training**, completing a self-learning cycle, resulting in a more capable, cognitively grounded foundation MLLM.

Following Korbak et al. (2023), we prioritize the comparison with various pre-training approaches. Specifically, we evaluate SICOG on both low-resolution and high-resolution MLLMs across diverse benchmarks. Extensive experimental results (Figure 1, right) demonstrate that SICOG produces stronger foundation models with enhanced multimodal cognition, significantly outperforming prevalent pre-training methods (Li et al., 2024a; Fang et al., 2024). In addition, SICOG enhances post-training performance and promotes continual self-improvement in newly constructed models. In summary, our contributions are three-fold:

- We propose SICOG, a self-learning framework that enhances MLLMs’ systematic cognition for constructing next-generation foundation MLLMs through multimodal pre-training with self-generated data.
- We introduce *Chain-of-Description*, a structured visual understanding mechanism that enables step-by-step interpretation of visual content to improve perceptual quality.
- We demonstrate SICOG’s effectiveness across various benchmarks on both low- and high-resolution MLLMs, significantly surpassing previous approaches.

108 **2 RELATED WORK**

110 **Multimodal Pre-Training.** Multimodal (vision-language) pre-training has proven highly effective
 111 in imparting multimodal knowledge and enhancing the perceptual capabilities of MLLMs by
 112 leveraging diverse, high-quality image-caption datasets (Lu et al., 2024a; Bai et al., 2023; Liu et al.,
 113 2024b). However, the construction of such datasets often depends on proprietary or open-source
 114 models to generate detailed captions (Chen et al., 2024a; Li et al., 2024d), or on expert visual
 115 models to extract fine-grained attributes (Peng et al., 2023), which are subsequently integrated into
 116 descriptive captions (Fang et al., 2024; Xu et al., 2024a; Sun et al., 2024). To reduce reliance on
 117 external annotations, we leverage the model’s inherent visual instruction-following and generalization
 118 capabilities to generate detailed caption data for self-improvement, similar to Fang et al. (2024); Deng
 119 et al. (2024). Beyond perception, we further enhance the model’s multimodal reasoning abilities by
 120 incorporating self-generated visual instruction-tuning data, including both direct answers and CoT
 121 formats. This enables a shift from focusing solely on perception to advancing cognitive capabilities.
 122 Detailed discussion is provided in Appendix D.

123 **3 METHODOLOGY: THE SICOG FRAMEWORK**

125 In this section, we introduce SICOG, a self-learning framework for constructing next-generation
 126 foundation MLLMs. We begin with a comprehensive overview in Section 3.1, then delve into the
 127 details of *Chain-of-Description* for systematic perception enhancement in Section 3.2, followed by
 128 structured CoT for systematic reasoning enhancement in Section 3.3. A comprehensive introduction
 129 to SICOG is available in Appendix B.

130 **3.1 OVERVIEW**

132 The goal of SICOG is to advance MLLMs by equipping them with rich multimodal knowledge and
 133 systematic cognitive capabilities—namely, systematic visual understanding (“how to observe”) and
 134 in-depth multimodal reasoning (“how to think”)—during multimodal pre-training, with minimal
 135 reliance on external annotations. As illustrated in Figure 2, SICOG operates through four key steps.

136 **Step 1: Developing Systematic Multimodal Cognition with Minimal Annotations.** We enhance
 137 the MLLM, \mathcal{M} (parameterized by θ), by fine-tuning it to systematically interpret and integrate
 138 multimodal information using minimal annotated data. This includes two main components:

139 • **Systematic multimodal perception.** To improve the MLLM’s ability to systematically observe
 140 and interpret images, we fine-tune \mathcal{M} using minimal high-quality image-captioning datasets
 141 $\mathcal{D}^{\text{Perception}}$, resulting in an enhanced perception model, $\mathcal{M}_0^{\text{Perception}}$. These datasets include images
 142 v , prompts x , step-by-step analyses s , and descriptions y , structured in two formats: Detailed
 143 Description (DD) and *Chain-of-Description* (CoD). Details of the *Chain-of-Description* strategy
 144 and data collection are provided in Section 3.2.

$$\mathcal{D}^{\text{Perception}} = \mathcal{D}_{\text{DD}}^{\text{Perception}} + \mathcal{D}_{\text{CoD}}^{\text{Perception}} = \{(v_i, x_i, y_i)\}_{i=1}^N + \{(v_i, x_i, s_i, y_i)\}_{i=1}^N, \quad (1)$$

145 where N is the number of training samples.

146 • **Systematic multimodal reasoning.** To improve reasoning, we fine-tune \mathcal{M} with minimal visual
 147 instruction-tuning datasets $\mathcal{D}^{\text{Reasoning}}$, resulting in $\mathcal{M}_0^{\text{Reasoning}}$. These datasets include images v ,
 148 questions q , intermediate step-by-step rationales r , and answers a , structured as Direct Answer
 149 (DA) and Chain-of-Thought (CoT). Details of data curation are provided in Section 3.3.

$$\mathcal{D}^{\text{Reasoning}} = \mathcal{D}_{\text{DA}}^{\text{Reasoning}} + \mathcal{D}_{\text{CoT}}^{\text{Reasoning}} = \{(v_i, q_i, a_i)\}_{i=1}^M + \{(v_i, q_i, r_i, a_i)\}_{i=1}^M, \quad (2)$$

150 where M is the number of samples.

151 **Step 2: Generating Candidate Captions and Responses for Pre-Training Data Collection.** We
 152 construct multimodal pre-training data by leveraging the improved models, $\mathcal{M}_0^{\text{Perception}}$ and $\mathcal{M}_0^{\text{Reasoning}}$,
 153 to generate candidate image captions and visual instruction responses. This step involves:

154 • **Image caption candidate generation.** Given a set of *unlabeled* images $\{v_k\}_{k=1}^K$, we prompt
 155 $\mathcal{M}_0^{\text{Perception}}$ (with policy $p_{\mathcal{M}_0^{\text{Perception}}}$) using two types of instructions to generate detailed descriptions
 156 and induce *Chain-of-Description* perception:

157 1. “Please generate a detailed caption of this image.” (x_{DD}).

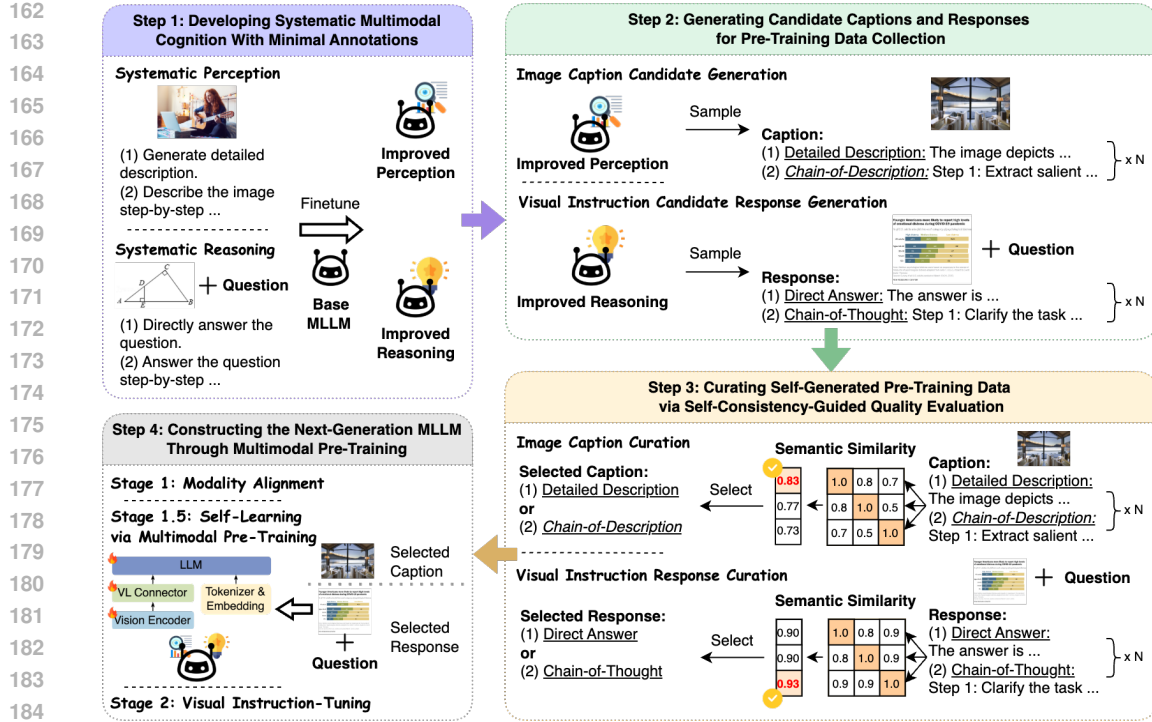


Figure 2: The SICOG framework comprises four steps: (i) Developing multimodal cognitive capabilities by finetuning an MLLM with minimal annotated image-captioning data (with *Chain-of-Description*) and visual instruction-tuning data (with structured Chain-of-Thought), enhancing systematic perception and reasoning (upper left). (ii) Generating candidate captions and responses for pre-training by sampling from the improved models (upper right). (iii) Curating self-generated pre-training data through self-consistency-guided quality evaluation, selecting the most semantically consistent candidates for learning (lower right). (iv) Constructing a next-generation foundation MLLM by performing multimodal pre-training on the curated data (lower left). For brevity, language ability preservation is omitted; see Figure 3 for the complete version.

2. "Please generate ... Describe the image step by step."
 (x_{CoD}) .

For each image v_k , $\mathcal{M}_0^{\text{Perception}}$ generates multiple candidate captions via sampling:

$$\{\hat{y}_k\} \sim p_{\mathcal{M}_0^{\text{Perception}}}(\cdot | v_k, x_{DD}), \{(\hat{s}_k, \hat{y}_k)\} \sim p_{\mathcal{M}_0^{\text{Perception}}}(\cdot | v_k, x_{CoD}), \quad (3)$$

where $\{\hat{y}_k\}$ is the set of detailed descriptions, and $\{(\hat{s}_k, \hat{y}_k)\}$ is the set of step-by-step analyses with descriptions. The resulting dataset includes captions in two formats.

- **Visual instruction candidate response generation.** For a set of *unlabeled* images $\{v_z\}_{z=1}^Z$ with corresponding questions q_z , we prompt $\mathcal{M}_0^{\text{Reasoning}}$ (with policy $p_{\mathcal{M}_0^{\text{Reasoning}}}$) using two types of instructions to generate direct answers and induce Chain-of-Thought reasoning:

1. "<original question>." (q_{DA}).
2. "<original question> Answer the question step by step." (q_{CoT}).

For each image v_z and question q_z , $\mathcal{M}_0^{\text{Reasoning}}$ produces multiple candidate responses:

$$\{\hat{a}_z\} \sim p_{\mathcal{M}_0^{\text{Reasoning}}}(\cdot | v_z, q_{DA}), \{(\hat{r}_z, \hat{a}_z)\} \sim p_{\mathcal{M}_0^{\text{Reasoning}}}(\cdot | v_z, q_{CoT}), \quad (4)$$

where $\{\hat{a}_z\}$ is the set of direct answers, and $\{(\hat{r}_z, \hat{a}_z)\}$ is the set of step-by-step rationales with answers. The resulting dataset includes responses in two formats.

Step 3: Curating Self-Generated Pre-Training Data via Self-Consistency-Guided Quality Evaluation. To ensure the quality of self-generated pre-training data across diverse tasks, we employ *self-consistency* (Wu et al., 2024; Li et al., 2024c) to evaluate candidate samples without external supervision. This method is based on the principle that *higher-quality candidates exhibit*

216 *greater semantic consistency*. The most consistent candidates are selected for further self-refinement
 217 during multimodal pre-training.

218 Specifically, we apply a semantic-similarity-guided self-consistency evaluation function, $f(\cdot)$. For
 219 each instance (e.g., an *unlabeled* image), it assesses the quality of candidates (e.g., candidate captions)
 220 by comparing each candidate against all others based on semantic similarity and selects the candidate
 221 with the highest consistency score, provided it exceeds a predefined threshold τ (i.e., otherwise, the
 222 instance and its candidates are skipped):

$$224 \quad f(\{c\}) = \arg \max_{c \in \{c\}} \frac{1}{N_{\text{cand}}} \sum_{j=1}^{N_{\text{cand}}} \text{sim}(c, c^{(j)}), \quad \text{s.t.} \quad \max_{c \in \{c\}} \frac{1}{N_{\text{cand}}} \sum_{j=1}^{N_{\text{cand}}} \text{sim}(c, c^{(j)}) \geq \tau, \quad (5)$$

227 where N_{cand} is the number of candidate samples being compared, and $\{c\}$ represents the candidate
 228 set. As illustrated in the lower-right part of Figure 2, we apply this method as follows:

- 230 • **Image caption curation.** For each image v_k , we apply $f(\cdot)$ to evaluate the quality of candidate
 231 captions by comparing each generated description \hat{y}_k against all others. The caption with the
 232 highest semantic consistency is selected as the final self-generated caption, resulting in a curated
 233 dataset of selected captions $\mathcal{D}_{\text{Selected}}^{\text{Perception}}$.
- 234 • **Visual instruction response curation.** For each image v_z and question q_z , $f(\cdot)$ evaluates candidate
 235 responses by comparing each generated answer \hat{a}_z against all others. The most consistent
 236 response is selected, resulting in a curated dataset $\mathcal{D}_{\text{Selected}}^{\text{Reasoning}}$.

238 In addition, to preserve language capabilities, we prompt the backbone LLM, \mathcal{M}_{LLM} , to generate
 239 candidate responses for *unlabeled* text-only instructions. These responses are then curated using
 240 a similar process, resulting in $\mathcal{D}_{\text{Selected}}^{\text{Language}}$. Combining all three curated datasets yields the final self-
 241 generated pre-training dataset $\mathcal{D}^{\text{Pre-training}}$.

242 **Step 4: Constructing the Next-Generation MLLM through Multimodal Pre-Training.** To build
 243 the next-generation foundation MLLM, we introduce an intermediate multimodal pre-training stage,
 244 Stage 1.5, within the standard two-stage training strategy, following (Liu et al., 2024b; Li et al., 2024a).
 245 This stage improves the MLLM using curated self-generated pre-training data. The complete training
 246 strategy consists of three stages, as shown in the lower left part in Figure 2: (i) **Stage 1: Modality**
 247 **alignment.** Align image features with the text embedding space. Following (Li et al., 2024a),
 248 only the vision-language connector is trained on image-text pairs during this stage. (ii) **Stage 1.5:**
 249 **Self-learning via multimodal pre-training.** Train the model on curated pre-training data $\mathcal{D}^{\text{Pre-training}}$
 250 to acquire multimodal knowledge and integrate systematic perception and reasoning. During this
 251 stage, all model components are fully trainable. (iii) **Stage 2: Visual instruction-tuning.** Fine-tune
 252 the model on instruction-tuning data to develop robust visual instruction-following capabilities. All
 253 model components remain fully trainable.

254 3.2 ENHANCING SYSTEMATIC PERCEPTION WITH *Chain-of-Description*

256 We introduce *Chain-of-Description* (CoD) to enable systematic perception, equipping the MLLM
 257 with the ability to logically analyze and describe visual information step by step (“how to observe”).
 258 This step-by-step approach enhances thorough visual interpretation. As shown in Figure 4 (left),
 259 *Chain-of-Description* consists of five sequential stages: (i) **Step 1: Extract salient content.** Identify
 260 the key elements that define the overall context and meaning of the image, laying the foundation
 261 for basic visual recognition. (ii) **Step 2: Analyze detailed information.** Focus on instance-level
 262 attributes, such as low-level and fine-grained details, e.g., “the guitar is a classic wooden brown with
 263 light-colored frets.” This step ensures a precise and detailed interpretation of the image. (iii) **Step**
 264 **3: Consider relational-level attributes.** Analyze interactions between elements and their spatial
 265 organization, e.g., “the person is seated on the bed,” leading to a richer and more comprehensive
 266 understanding of visual relationships. (iv) **Step 4: Examine marginal or peripheral content.** Pay
 267 attention to less prominent or background details, e.g., “the dresser in the background,” to ensure
 268 no important information is overlooked. (v) **Step 5: Organize all observations.** Synthesize all
 269 findings into a cohesive, detailed description, enabling comprehensive coverage and holistic image
 understanding. Due to space constraints, details regarding the **data preparation** for minimally
 annotated CoD data are provided in Appendix B.1.

270 3.3 IMPROVING SYSTEMATIC REASONING WITH STRUCTURED CHAIN-OF-THOUGHT
271

272 We adopt structured CoT (Xu et al., 2025) to enhance MLLMs’ systematic reasoning capabilities. As
273 shown in Figure 4 (right), this approach decomposes complex multimodal tasks into logical steps,
274 enabling progressive analysis and reasoning. The structured CoT process follows four key stages: (i)
275 **Step 1: Clarify the task objective.** Identify the problem’s requirements to establish a foundational
276 understanding. (ii) **Step 2: Extract crucial visual information.** Identify relevant visual elements to
277 inform the reasoning process. (iii) **Step 3: Generate detailed reasoning.** Construct a logical chain
278 of intermediate steps based on the visual and textual context. (iv) **Step 4: Conclude with an answer.**
279 Synthesize the reasoning steps into a coherent and accurate response. Due to space limitations, details
280 on the **data preparation** for minimally annotated CoT data are provided in Appendix B.2.

281 4 EXPERIMENTS
282

283 4.1 EXPERIMENTAL SETUP

284 **Datasets and Evaluation Metrics.** We evaluate the efficacy of SICOG on the following well-
285 established benchmarks, using the open-source evaluation toolkit VLMEvalKit (Duan et al., 2024):
286 (i) **Multimodal Comprehensive Understanding:** MMStar (Chen et al., 2024c), MMBench (Liu
287 et al., 2024d), MMVet (Yu et al., 2024b) (report accuracy). (ii) **Hallucination:** POPE (Li et al., 2023)
288 (report F1 score). (iii) **Chart/Table Understanding:** OCRBench (Liu et al., 2024e), DocVQA (Tito
289 et al., 2021), ChartQA (Masry et al., 2022) (report accuracy). (iv) **Knowledge-Oriented Tasks:**
290 MathVista (Lu et al., 2024b), ScienceQA (Lu et al., 2022), AI2D (Kembhavi et al., 2016) (report
291 accuracy). (v) **Real-World Understanding:** RealWorldQA (X.AI, 2024) (report accuracy).

292 **Compared Methods.** We compare SICOG against the following representative MLLM pre-training
293 approaches (as discussed in Section 2). Differences are considered significant at $p < 0.01$: (i)
294 **Strong-to-Weak Distillation (Perception)** (Li et al., 2024a): Pre-training with re-caption data
295 containing detailed descriptions (DD) generated by stronger models. (ii) **Multi-Agent Collaboration**
296 (**Perception**) (Fang et al., 2024): Pre-training with re-caption data containing detailed descriptions
297 and fine-grained attributes (DD-FGA) generated by base and expert models. Due to space limitations,
298 we provide **Implementation Details** in Appendix M.

299 4.2 CAN SELF-IMPROVED SYSTEMATIC COGNITION YIELD NEXT-GENERATION
300 FOUNDATION MLLMs?

301 Table 1 presents the comprehensive evaluation results. Following Korbak et al. (2023), we prioritize
302 comparisons with various pre-training approaches rather than emphasizing state-of-the-art (SOTA)
303 performance. The key observations are summarized as follows:

305 **SICOG yields next-generation foundation MLLMs with self-improved cognitive capabilities.**
306 SICOG consistently improves both high-resolution and low-resolution foundation MLLMs across di-
307 verse tasks, achieving gains of 2%–3.5% on MMStar for comprehensive tasks, 2%–3% on perception
308 tasks (e.g., DocVQA and ChartQA), and 2%–4% on reasoning tasks (e.g., ScienceQA and AI2D).

309 **Systematic perception through self-learning strengthens foundation MLLMs.** SICOG (Percep-
310 tion), which leverages self-generated captions with detailed descriptions and *Chain-of-Description*,
311 achieves comparable or superior accuracy across benchmarks relative to strong-to-weak distillation
312 and multimodal collaboration methods. Unlike these alternatives, which heavily rely on extensive
313 external annotations, SICOG reduces this dependence through self-learning.

314 **Integrating systematic reasoning into pre-training proves more effective than prioritizing**
315 **perception alone.** SICOG (Perception + Reasoning) boosts multimodal reasoning, surpassing
316 perception-only methods by 2.5%–4% on ScienceQA while preserving strong perception capabilities.
317 Notably, perception-only pre-training degrades performance on hallucination tasks (a 0.5%–1% drop
318 on POPE), whereas systematic reasoning mitigates this issue and maintains robustness. Incorporating
319 self-generated text-only instruction-tuning data during pre-training further enhances performance,
320 especially for high-resolution MLLMs. This observation aligns with findings in (Lu et al., 2024a).

321 **Stronger foundation MLLMs enable more effective self-improvement.** SICOG achieves greater
322 performance gains when applied to LLaVA-Qwen2-7B-UHD (higher baseline capabilities) compared
323 to LLaVA-Llama3.1-8B-UHD (lower baseline capabilities), showing that base model performance
significantly influences self-improvement potential, with stronger MLLMs yielding better results.

324
 325 Table 1: Evaluation results on eight benchmarks (direct answer inference). *The only difference*
 326 *between the compared methods is the pre-training data utilized in Stage 1.5 (see details in Step 4 of*
 327 *Section 3).* Results marked with an asterisk (*) are cited from the OpenVLM Leaderboard (Duan
 328 et al., 2024). Some results are provided in Appendix P.

| 329 Method | 330 Train Data | 331 Comprehensive | 332 Hallu. | 333 Chart/Table | 334 Knowledge | | | | |
|--|---|----------------------|---------------|--------------------|------------------|---------------|--------------|-----------------|--------------|
| | 335 Stage 1.5 | 336 MMBen. | 337 MMStar | 338 POPE | 339 DocV. | 340 Chart. | 341 Math. | 342 Science. | 343 AI2D |
| <i>Open-Sourced Models (For holistic analysis, not for comparison)</i> | | | | | | | | | |
| VITA-1.0-Mixtral-8x7B* (Fu et al., 2024a) | - | - | 46.60 | - | - | - | 44.50 | - | 72.80 |
| LLaVA-v1.5-13B* (Liu et al., 2024a) | - | 69.20 | 34.30 | 88.40 | - | 18.20 | 27.70 | 72.60 | 61.10 |
| ShareGPT4V-13B* (Chen et al., 2024b) | - | 69.80 | 38.30 | 87.50 | - | 24.60 | 29.40 | 72.60 | 61.40 |
| Molmo-7B-O* (Deitke et al., 2024) | - | 72.20 | 50.10 | 86.70 | - | 36.50 | 43.90 | 88.80 | 75.70 |
| Eagle-X5-13B* (Shi et al., 2024) | - | 72.60 | 43.70 | 89.80 | - | 69.60 | 40.80 | 71.80 | 77.00 |
| CogVLM2-19B-Chat* (Chen et al., 2025) | - | 73.90 | 50.50 | 83.40 | - | 33.00 | 38.70 | 90.20 | 73.40 |
| LLaVA-NeXT-8B* (Li et al., 2024a) | - | 74.80 | 43.90 | 87.10 | - | 68.70 | 37.70 | 73.10 | 72.80 |
| Cambrrian-1-8B* (Tong et al., 2024) | - | 74.60 | 50.70 | 86.40 | - | 72.60 | 48.10 | 81.00 | 74.60 |
| XGen-MM-Instruct-Interleave-v1.5* (Xue et al., 2024) | Sufficient high-quality multimodal data | 78.30 | 48.40 | 87.20 | - | - | 40.60 | 88.30 | 74.20 |
| Janus-Pro-7B* (Chen et al., 2025) | Sufficient high-quality multimodal data | 62.60 | 46.50 | 78.90 | - | - | 42.50 | 83.20 | 68.10 |
| DeepSeek-VL-7B* (Lu et al., 2024a) | Sufficient high-quality multimodal data | 73.80 | 40.50 | 85.60 | - | 59.10 | 37.20 | 80.90 | 65.30 |
| VILA1.5-13B* (Lin et al., 2024) | Sufficient high-quality multimodal data | 74.40 | 44.20 | 85.00 | - | - | 42.30 | 79.10 | 69.90 |
| Low-Resolution | | | | | | | | | |
| <i>Base Model</i> | | | | | | | | | |
| LLaVA-Qwen2-7B (Liu et al., 2023) | - | 74.44 | 46.67 | 84.55 | 50.62 | 52.72 | 38.00 | 74.91 | 73.77 |
| <i>Strong-to-Weak Distillation (Perception)</i> | | | | | | | | | |
| LLaVA-NeXT-34B-LLaVA-Qwen2-7B | 118k Caption w/ DD by LLaVA-NeXT-34B | 76.18 | 46.73 | 83.72 | 51.26 | 52.68 | 36.60 | 75.56 | 74.38 |
| Qwen2-VL-72B-Instruct-LLaVA-Qwen2-7B | 118k Caption w/ DD by Qwen2-VL-72B-Instruct | 75.84 | 48.20 | 83.84 | 50.85 | 52.56 | 36.10 | 76.15 | 74.87 |
| <i>Multi-Agent Collaboration (Perception)</i> | | | | | | | | | |
| Multi-Experts-LLaVA-Qwen2-7B | 118k Caption w/ DD-FGA by base and expert models | 76.01 | 47.60 | 84.12 | 51.06 | 53.36 | 38.90 | 75.46 | 74.97 |
| <i>Self-Improving Cognition (Perception & Reasoning)</i> | | | | | | | | | |
| SICOG-LLaVA-Qwen2-7B (Perception) | Self-generated 118k caption w/ DD&CoD | 75.34 | 48.27 | 83.89 | 50.83 | 54.88 | 38.50 | 74.71 | 75.13 |
| SICOG-LLaVA-Qwen2-7B (Perception, Reasoning) | Self-generated 118k caption w/ DD&CoD, 45k VQA w/ DA&CoT | 76.01 | 48.67 | 84.10 | 52.70 | 55.20 | 38.10 | 78.88 | 76.78 |
| SICOG-LLaVA-Qwen2-7B (Perception, Reasoning, Language) | Self-generated 118k caption w/ DD&CoD, 45k VQA w/ DA&CoT, 50k textual QA | 75.45 | 48.60 | 84.35 | 52.52 | 54.48 | 38.80 | 77.44 | 76.20 |
| High-Resolution | | | | | | | | | |
| <i>Base Model</i> | | | | | | | | | |
| LLaVA-Qwen2-7B-UHD (Guo et al., 2024) | - | 77.63 | 48.93 | 87.31 | 70.18 | 69.96 | 38.90 | 77.29 | 74.94 |
| <i>Strong-to-Weak Distillation (Perception)</i> | | | | | | | | | |
| LLaVA-NeXT-34B-LLaVA-Qwen2-7B-UHD | 118k Caption w/ DD by LLaVA-NeXT-34B | 77.75 | 50.60 | 86.46 | 71.20 | 71.56 | 36.90 | 78.38 | 76.00 |
| Qwen2-VL-72B-Instruct-LLaVA-Qwen2-7B-UHD | 118k Caption w/ DD by Qwen2-VL-72B-Instruct | 77.75 | 51.87 | 86.43 | 71.05 | 72.40 | 38.30 | 79.42 | 76.52 |
| <i>Multi-Agent Collaboration (Perception)</i> | | | | | | | | | |
| Multi-Experts-LLaVA-Qwen2-7B-UHD | 118k Caption w/ DD-FGA by base and expert models | 77.97 | 49.87 | 86.48 | 71.27 | 71.80 | 37.90 | 77.79 | 76.62 |
| <i>Self-Improving Cognition (Perception & Reasoning)</i> | | | | | | | | | |
| SICOG-LLaVA-Qwen2-7B-UHD (Perception) | Self-generated 118k caption w/ DD&CoD | 78.08 | 51.60 | 87.03 | 72.42 | 73.04 | 39.50 | 77.34 | 77.59 |
| SICOG-LLaVA-Qwen2-7B-UHD (Perception, Reasoning) | Self-generated 118k caption w/ DD&CoD, 45k VQA w/ DA&CoT | 77.19 | 50.13 | 87.32 | 73.70 | 73.12 | 39.50 | 79.23 | 77.91 |
| SICOG-LLaVA-Qwen2-7B-UHD (Perception, Reasoning, Language) | Self-generated 118k caption w/ DD&CoD, 45k VQA w/ DA&CoT, 50k textual QA | 77.80 | 52.47 | 87.84 | 73.05 | 72.24 | 41.40 | 79.42 | 78.40 |
| LLaVA-Llama3.1-8B-UHD | | | | | | | | | |
| SICOG-LLaVA-Llama3.1-8B-UHD (Perception) | - | 72.14 | 43.93 | 87.85 | 64.32 | 64.64 | 33.90 | 74.96 | 71.70 |
| SICOG-LLaVA-Llama3.1-8B-UHD (Perception, Reasoning) | Self-generated 118k caption w/ DD&CoD | 71.92 | 44.80 | 87.37 | 65.09 | 64.96 | 35.70 | 74.52 | 71.11 |
| SICOG-LLaVA-Llama3.1-8B-UHD (Perception, Reasoning, Language) | Self-generated 118k caption w/ DD&CoD, 45k VQA w/ DA&CoT | 72.03 | 43.20 | 87.38 | 65.78 | 65.56 | 35.90 | 76.15 | 72.05 |
| SICOG-LLaVA-Llama3.1-8B-UHD (Perception, Reasoning, Language) | Self-generated 118k caption w/ DD&CoD, 45k VQA w/ DA&CoT, 50k textual QA | 72.31 | 43.07 | 87.21 | 64.95 | 65.00 | 33.30 | 75.56 | 70.76 |

375 Additionally, **SICOG** achieves leading performance in fine-grained evaluations of six core capabilities (Appendix K). Scaling up self-generated data further enhances **SICOG**'s performance (Appendix G). **SICOG** remains effective when varying recaptioned images (Appendix H) and contributes to next-generation foundation MLLMs through continuous cognitive self-improvement

(Appendix I). These findings collectively demonstrate SICOG’s effectiveness in advancing multimodal cognitive abilities in MLLMs.

4.3 CAN SICOG FACILITATE A STRONGER REASONING FOUNDATION FOR PROTOTYPING CHAIN-OF-THOUGHT REASONERS DURING POST-TRAINING?

Table 2: Evaluation results of fine-tuning foundation MLLMs to build a CoT reasoner via supervised fine-tuning on 35k CoT reasoning examples (curated in Section 3). P., R., and L. refer to perception, reasoning, and language, respectively.

| Method | Inference | Comprehensive | | Hallu. Chart/Table | | Knowledge | | | | |
|--|-----------|---------------|--------------|--------------------|--------------|--------------|--------------|--------------|--------------|--------------|
| | | MMBench | MMStar | MMVet | POPE | DocV. | Chart. | Math. | Science. | AI2D |
| Base Model | | | | | | | | | | |
| LLaVA-Qwen2-7B-UHD | Direct | 77.63 | 48.93 | 38.26 | 87.31 | 70.18 | 69.96 | 38.90 | 77.29 | 74.94 |
| LLaVA-Qwen2-7B-UHD + Finetune w/ 35k VQA (CoT) | CoT | 72.09 | 49.87 | 41.06 | 85.32 | 69.08 | 77.48 | 44.90 | 84.88 | 72.12 |
| Self-Improving Cognition | | | | | | | | | | |
| SICOG-LLaVA-Qwen2-7B-UHD (P., R., L.) + Finetune w/ 35k VQA (CoT) | CoT | 71.97 | 51.00 | 47.29 | 86.34 | 70.76 | 79.24 | 45.70 | 85.77 | 74.09 |

We validate the efficacy of SICOG in strengthening the reasoning foundation for constructing CoT reasoners during post-training. Specifically, we adopt a supervised fine-tuning approach, refining both the base model, LLaVA-Qwen2-7B-UHD, and SICOG-LLaVA-Qwen2-7B-UHD on the 35k CoT reasoning dataset curated in Section 3.

SICOG establishes a stronger foundation for prototyping a CoT reasoner. Table 2 demonstrates that post-training the SICOG-LLaVA-Qwen2-7B-UHD outperforms the post-trained baseline across most benchmarks, with up to 6% higher accuracy on MMVet.

Solely enhancing CoT reasoning may compromise perception abilities. We observe a significant performance drop on MMBench, which assesses a diverse range of perception tasks. This suggests that prioritizing CoT reasoning in MLLMs can inadvertently impair perception capabilities, underscoring the trade-off between reasoning and perception and the need for balanced optimization. Moreover, we provide an in-depth analysis (both quantitative and qualitative) of how SICOG enhances the reasoning capabilities of foundation MLLMs in Appendix F.

4.4 CAN PREFERENCE LEARNING SUPPORT SICOG’S SYSTEMATIC PERCEPTION AND REASONING DEVELOPMENT?

Table 3: Evaluation results of different training methods for developing perception and reasoning in LLaVA-Qwen2-7B during Step 1 of SICOG (post-training optimization, Section 3).

| Method | Capability Development | Comprehensive | | Hallu. Chart & Table | | Knowledge | | | | |
|--|--|--------------------------------|--------------------------------|--------------------------------|--------------------------------|--------------------------------|--------------------------------|--------------------------------|-------------------------|--------------------------------|
| | | MMBench | MMStar | MMVet | POPE | DocV. | Chart. | Math. | Science. | AI2D |
| Base Model | | | | | | | | | | |
| LLaVA-Qwen2-7B | - | 74.44 | 46.67 | 38.85 | 84.55 | 50.62 | 52.72 | 38.00 | 74.91 | 73.77 |
| Self-Improving Cognition | | | | | | | | | | |
| SICOG-LLaVA-Qwen2-7B (Per., Rea., Lan.) | SFT (Per., Rea.) DPO (Per.), SFT (Rea.) DPO (Per., Rea.) | 75.45 76.18 74.83 | 48.60 48.40 49.00 | 37.84 38.72 38.90 | 84.35 83.53 84.85 | 52.52 52.20 52.54 | 54.48 54.80 55.64 | 38.80 39.20 41.00 | 77.44 77.49 76.20 | 76.20 75.78 76.33 |

We explore the application of preference learning to enhance MLLMs’ multimodal perception and reasoning capabilities during Step 1 of SICOG (post-training optimization, Section 3). Specifically, we construct preference caption pairs by selecting high-quality captions from the annotated caption dataset (Section 3) as preferred captions and pairing them with corresponding low-quality (dispreferred) captions. The low-quality captions are generated by corrupting the associated images (details provided in Appendix E). We fine-tune the MLLM on these caption preference pairs using the Direct Preference Optimization (DPO) algorithm (Rafailov et al., 2023) to initialize systematic perception capabilities. Similarly, we extend preference learning to foster systematic reasoning development.

Preference learning is more effective than supervised fine-tuning for systematic perception and reasoning development. Preference learning with DPO consistently surpasses standard supervised

432 fine-tuning across all benchmarks for initializing systematic perception and reasoning in SICOG.
 433 For example, on MathVista, preference learning improves accuracy by approximately 2% on the
 434 low-resolution model LLaVA-Qwen2-7B, which is particularly challenging to enhance due to inherent
 435 visual perception limitations. These results underscore the importance of learning not only from
 436 correct examples but also from avoiding mistakes, thereby fostering more robust skill development.
 437 We provide a detailed analysis in Appendix E.

439 4.5 How Do *Chain-of-Description* AND CHAIN-OF-THOUGHT IMPROVE COGNITION?

441 Table 4: Evaluation of re-captioning quality comparing the perception-enhanced models fine-tuned
 442 on curated caption data in three formats: detailed description (Detailed D), *Chain-of-Description*
 443 (CoD), and their combination (Section 3). Metrics (rated 1-5): salient content, fine-grained details,
 444 relational attributes, peripheral content, faithfulness, and world knowledge. “Caption”: standard
 445 format; “Multi.”: CoD step-by-step format (see Table 11 in Appendix M for details). Complete
 446 results in Appendix J.

| 448 Method | # Avg. 449 Tokens | Systematic Perception | | | | General Performance | |
|---|----------------------|-----------------------|-------------|-------------|-------------|---------------------|-------------|
| | | Sali. | Fine-Grain. | Rela. | Peri. | Faith. | Know. |
| 450 LLaVA-Qwen2-7B-UHD | 135.08 | 4.77 | 4.30 | 3.99 | 3.81 | 4.41 | 3.84 |
| 451 + Finetune w/ Detailed D | 140.73 | 4.71 | 4.52 | 3.92 | 3.91 | 4.20 | 3.77 |
| 452 + Finetune w/ CoD (Caption) | 126.93 | 4.78 | 4.58 | 4.11 | 3.90 | 4.57 | 3.93 |
| 453 + Finetune w/ CoD (Multi.) | 453.13 | 4.82 | 4.80 | 4.74 | 4.29 | 4.57 | 4.01 |
| 454 + Finetune w/ Detailed D & CoD (Detailed D) | 136.50 | 4.76 | 4.67 | 4.01 | 3.82 | 4.51 | 3.88 |
| 455 + Finetune w/ Detailed D & CoD (CoD Multi.) | 453.26 | 4.91 | 4.87 | 4.78 | 4.32 | 4.71 | 4.05 |
| 456 LLaVA-NeXT-34B (Liu et al., 2024b) | 206.50 | 4.77 | 4.51 | 4.04 | 3.95 | 4.59 | 4.12 |

457 **How Does *Chain-of-Description* Facilitate Multimodal Perception? (Quantitative Analysis.)**
 458 We analyze captions for 100 images randomly sampled from BLIP-558k (Li et al., 2022), which is
 459 used as unlabeled image captioning data in Section 4. These captions are generated by perception-
 460 enhanced models fine-tuned on annotated caption data in three formats: detailed description (Detailed
 461 D), *Chain-of-Description* (CoD), and their combination (as implemented in SICOG, described in
 462 Section 3). Using GPT-4 with the prompt shown in Table 21, we evaluate six key dimensions. For a
 463 holistic analysis, we also include LLaVA-NeXT-34B, a leading open-source MLLM known for its
 464 strong captioning capabilities (Li et al., 2024a). Table 9 shows that the base model, regardless of
 465 resolution, consistently underperforms in salient content, fine-grained details, relational attributes,
 466 and peripheral content. These results highlight the importance of the four-step perception analysis
 467 design used in CoD.

468 ***Chain-of-Description* shows strong efficacy in facilitating systematic perception across six key
 469 dimensions.** Perception-enhanced models fine-tuned with *Chain-of-Description* outperform those
 470 trained on detailed descriptions in both single-step (caption-only) and multi-step formats. Notably,
 471 their combination achieves the highest evaluation scores, surpassing LLaVA-NeXT-34B in five of the
 472 six dimensions. Furthermore, *Chain-of-Description* generates the longest average caption lengths
 473 (approximately 430–450 tokens), indicating a robust perceptual capacity. Additional analysis is
 474 provided in Appendix L. Due to space constraints, we provide **the qualitative analysis of *Chain-of-Description* and a detailed discussion of structured Chain-of-Thought** in Appendix J.

476 5 CONCLUSION

478 We present SICOG, a self-learning framework for constructing next-generation foundation MLLMs
 479 by injecting multimodal knowledge and enhancing systematic cognition through multimodal pre-
 480 training with self-generated data. Extensive experiments demonstrate that SICOG produces a next-
 481 generation MLLM with significantly enhanced cognitive abilities, outperforming existing pre-training
 482 approaches across a wide range of benchmarks. Notably, we empirically validate that integrating
 483 pre-training with downstream mechanisms—such as post-training optimization and inference-time
 484 computation—enables more effective model development, establishing a foundation for a complete
 485 self-improving paradigm. For future work, we aim to incorporate embodied experiential data (Zhao
 et al., 2025) to further enhance real-world application capabilities.

486 ETHICS STATEMENT
487

488 Throughout our research, we have adhered to ethical guidelines that prioritize privacy, fairness, and
489 the well-being of all individuals and groups. All benchmark datasets used in this study are intended
490 solely for research purposes and do not contain any personally identifiable information, thereby
491 safeguarding user privacy. To elicit *Chain-of-Description* data, we carefully designed prompts to
492 avoid language that could be biased or discriminatory toward any individual or group. These measures
493 were implemented to minimize potential negative impacts on users. Furthermore, all self-generated
494 datasets were manually verified to ensure they are free from offensive content, misinformation, and
495 personally identifiable information. To ensure ethical integrity, prompts used for data generation were
496 carefully designed to exclude biased or discriminatory language. All generated data was manually
497 reviewed to confirm it contains no offensive material, misinformation, or personally identifiable
498 information.

499 REPRODUCIBILITY STATEMENT
500

501 We provide all necessary implementation details in Section 4 and Appendix M. The source code
502 and raw data are included in the supplementary materials, along with detailed instructions in the
503 README .md file. All results are easily reproducible.

504 REFERENCES
505

506 Jinze Bai, Shuai Bai, Shusheng Yang, Shijie Wang, Sinan Tan, Peng Wang, Junyang Lin, Chang Zhou,
507 and Jingren Zhou. Qwen-VL: A versatile vision-language model for understanding, localization,
508 text reading, and beyond. *arXiv preprint arXiv:2308.12966*, 2023.

509 Zechen Bai, Pichao Wang, Tianjun Xiao, Tong He, Zongbo Han, Zheng Zhang, and Mike Zheng Shou.
510 Hallucination of multimodal large language models: A survey. *arXiv preprint arXiv:2404.18930*,
511 2024.

512 Florian Bordes, Richard Yuanzhe Pang, Anurag Ajay, Alexander C Li, Adrien Bardes, Suzanne
513 Petryk, Oscar Mañas, Zhiqiu Lin, Anas Mahmoud, Bargav Jayaraman, et al. An introduction to
514 vision-language modeling. *arXiv preprint arXiv:2405.17247*, 2024.

515 Soravit Changpinyo, Piyush Sharma, Nan Ding, and Radu Soricut. Conceptual 12m: Pushing
516 web-scale image-text pre-training to recognize long-tail visual concepts. In *Proceedings of the
517 IEEE/CVF conference on computer vision and pattern recognition*, pp. 3558–3568, 2021.

518 Guiming Hardy Chen, Shunian Chen, Ruifei Zhang, Junying Chen, Xiangbo Wu, Zhiyi Zhang,
519 Zhihong Chen, Jianquan Li, Xiang Wan, and Benyou Wang. Allava: Harnessing gpt4v-synthesized
520 data for lite vision-language models. *arXiv preprint arXiv:2402.11684*, 2024a.

521 Lin Chen, Jinsong Li, Xiaoyi Dong, Pan Zhang, Conghui He, Jiaqi Wang, Feng Zhao, and Dahu Lin.
522 Sharegpt4v: Improving large multi-modal models with better captions. In *European Conference
523 on Computer Vision*, pp. 370–387. Springer, 2024b.

524 Lin Chen, Jinsong Li, Xiaoyi Dong, Pan Zhang, Yuhang Zang, Zehui Chen, Haodong Duan, Jiaqi
525 Wang, Yu Qiao, Dahu Lin, et al. Are we on the right way for evaluating large vision-language
526 models? *Advances in Neural Information Processing Systems*, 37, 2024c.

527 Qiguang Chen, Libo Qin, Jin Zhang, Zhi Chen, Xiao Xu, and Wanxiang Che. M3cot: A novel
528 benchmark for multi-domain multi-step multi-modal chain-of-thought. In *Proceedings of the 62nd
529 Annual Meeting of the Association for Computational Linguistics (Volume 1: Long Papers)*, pp.
530 8199–8221, 2024d.

531 Xiaokang Chen, Zhiyu Wu, Xingchao Liu, Zizheng Pan, Wen Liu, Zhenda Xie, Xingkai Yu, and
532 Chong Ruan. Janus-pro: Unified multimodal understanding and generation with data and model
533 scaling. *arXiv preprint arXiv:2501.17811*, 2025.

534 Kanzhi Cheng, Yantao Li, Fangzhi Xu, Jianbing Zhang, Hao Zhou, and Yang Liu. Vision-language
535 models can self-improve reasoning via reflection. *arXiv preprint arXiv:2411.00855*, 2024.

540 Matt Deitke, Christopher Clark, Sangho Lee, Rohun Tripathi, Yue Yang, Jae Sung Park, Moham-
 541 madreza Salehi, Niklas Muennighoff, Kyle Lo, Luca Soldaini, et al. Molmo and pixmo: Open
 542 weights and open data for state-of-the-art multimodal models. *arXiv preprint arXiv:2409.17146*,
 543 2024.

544

545 Yihe Deng, Pan Lu, Fan Yin, Ziniu Hu, Sheng Shen, Quanquan Gu, James Y Zou, Kai-Wei Chang, and
 546 Wei Wang. Enhancing large vision language models with self-training on image comprehension.
 547 *Advances in Neural Information Processing Systems*, 37:131369–131397, 2024.

548

549 Yuhao Dong, Zuyan Liu, Hai-Long Sun, Jingkang Yang, Winston Hu, Yongming Rao, and Ziwei Liu.
 550 Insight-v: Exploring long-chain visual reasoning with multimodal large language models. *arXiv*
 551 *preprint arXiv:2411.14432*, 2024.

552

553 Haodong Duan, Junming Yang, Yuxuan Qiao, Xinyu Fang, Lin Chen, Yuan Liu, Xiaoyi Dong, Yuhang
 554 Zang, Pan Zhang, Jiaqi Wang, et al. Vlmevalkit: An open-source toolkit for evaluating large
 555 multi-modality models. In *Proceedings of the 32nd ACM international conference on multimedia*,
 556 pp. 11198–11201, 2024.

557

558 Yunhao Fang, Ligeng Zhu, Yao Lu, Yan Wang, Pavlo Molchanov, Jan Kautz, Jang Hyun Cho, Marco
 559 Pavone, Song Han, and Hongxu Yin. Vila2: Vila augmented vila. *arXiv preprint arXiv:2407.17453*,
 560 2024.

561

562 Kaituo Feng, Kaixiong Gong, Bohao Li, Zonghao Guo, Yibing Wang, Tianshuo Peng, Benyou
 563 Wang, and Xiangyu Yue. Video-r1: Reinforcing video reasoning in mllms. *arXiv preprint*
 564 *arXiv:2503.21776*, 2025.

565

566 Chaoyou Fu, Haojia Lin, Zuwei Long, Yunhang Shen, Meng Zhao, Yifan Zhang, Shaoqi Dong, Xiong
 567 Wang, Di Yin, Long Ma, et al. Vita: Towards open-source interactive omni multimodal llm. *arXiv*
 568 *preprint arXiv:2408.05211*, 2024a.

569

570 Ling Fu, Biao Yang, Zhebin Kuang, Jiajun Song, Yuzhe Li, Linghao Zhu, Qidi Luo, Xinyu Wang, Hao
 571 Lu, Mingxin Huang, et al. Ocrbench v2: An improved benchmark for evaluating large multimodal
 572 models on visual text localization and reasoning. *arXiv preprint arXiv:2501.00321*, 2024b.

573

574 Kanishk Gandhi, Ayush Chakravarthy, Anikait Singh, Nathan Lile, and Noah D Goodman. Cognitive
 575 behaviors that enable self-improving reasoners, or, four habits of highly effective stars. *arXiv*
 576 *preprint arXiv:2503.01307*, 2025.

577

578 Aaron Grattafiori, Abhimanyu Dubey, Abhinav Jauhri, Abhinav Pandey, Abhishek Kadian, Ahmad
 579 Al-Dahle, Aiesha Letman, Akhil Mathur, Alan Schelten, Alex Vaughan, et al. The llama 3 herd of
 580 models. *arXiv preprint arXiv:2407.21783*, 2024.

581

582 Daya Guo, Dejian Yang, Haowei Zhang, Junxiao Song, Ruoyu Zhang, Runxin Xu, Qihao Zhu,
 583 Shirong Ma, Peiyi Wang, Xiao Bi, et al. Deepseek-r1: Incentivizing reasoning capability in llms
 584 via reinforcement learning. *arXiv preprint arXiv:2501.12948*, 2025.

585

586 Zonghao Guo, Ruyi Xu, Yuan Yao, Junbo Cui, Zanlin Ni, Chunjiang Ge, Tat-Seng Chua, Zhiyuan
 587 Liu, and Gao Huang. Llava-uhd: An lmm perceiving any aspect ratio and high-resolution images.
 588 In *European Conference on Computer Vision*, pp. 390–406, 2024.

589

590 Yunzhuo Hao, Jiawei Gu, Huichen Will Wang, Linjie Li, Zhengyuan Yang, Lijuan Wang, and
 591 Yu Cheng. Can mllms reason in multimodality? emma: An enhanced multimodal reasoning
 592 benchmark. *arXiv preprint arXiv:2501.05444*, 2025.

593

594 Aaron Hurst, Adam Lerer, Adam P Goucher, Adam Perelman, Aditya Ramesh, Aidan Clark, AJ Os-
 595 trow, Akila Welihinda, Alan Hayes, Alec Radford, et al. Gpt-4o system card. *arXiv preprint*
 596 *arXiv:2410.21276*, 2024.

597

598 Aniruddha Kembhavi, Mike Salvato, Eric Kolve, Minjoon Seo, Hannaneh Hajishirzi, and Ali Farhadi.
 599 A diagram is worth a dozen images. In *Computer Vision–ECCV 2016: 14th European Conference*,
 600 *Amsterdam, The Netherlands, October 11–14, 2016, Proceedings, Part IV* 14, pp. 235–251.
 601 Springer, 2016.

594 Nasima Khatun, Prosanta Paul, Sridip Chatterjee, and Sudip Sundar Das. Physical activity and
 595 neurocognitive health: A narrative review. *International Journal of Research Pedagogy and*
 596 *Technology in Education and Movement Sciences*, 12(02):94–101, 2023.

597

598 Tomasz Korbak, Kejian Shi, Angelica Chen, Rasika Vinayak Bhalerao, Christopher Buckley, Jason
 599 Phang, Samuel R Bowman, and Ethan Perez. Pretraining language models with human preferences.
 600 In *International Conference on Machine Learning*, pp. 17506–17533. PMLR, 2023.

601 Zhengfeng Lai, Haotian Zhang, Wentao Wu, Haoping Bai, Aleksei Timofeev, Xianzhi Du, Zhe Gan,
 602 Jiulong Shan, Chen-Nee Chuah, Yinfei Yang, et al. From scarcity to efficiency: Improving clip
 603 training via visual-enriched captions. *OpenReview: gdJTPCQxXJ*, 2023.

604

605 Zhengfeng Lai, Haotian Zhang, Bowen Zhang, Wentao Wu, Haoping Bai, Aleksei Timofeev, Xianzhi
 606 Du, Zhe Gan, Jiulong Shan, Chen-Nee Chuah, et al. Veclip: Improving clip training via visual-
 607 enriched captions. In *European Conference on Computer Vision*, pp. 111–127. Springer, 2024.

608 Chankyu Lee, Rajarshi Roy, Mengyao Xu, Jonathan Raiman, Mohammad Shoeybi, Bryan Catanzaro,
 609 and Wei Ping. Nv-embed: Improved techniques for training llms as generalist embedding models.
 610 *arXiv preprint arXiv:2405.17428*, 2024.

611 Bo Li, Hao Zhang, Kaichen Zhang, Dong Guo, Yuanhan Zhang, Renrui Zhang,
 612 Feng Li, Ziwei Liu, and Chunyuan Li. Llava-next: What else influences vi-
 613 sual instruction tuning beyond data? [https://llava-vl.github.io/blog/](https://llava-vl.github.io/blog/2024-05-25-llava-next-ablations/)
 614 2024-05-25-llava-next-ablations/, May 2024a.

615

616 Chunyuan Li, Zhe Gan, Zhengyuan Yang, Jianwei Yang, Linjie Li, Lijuan Wang, Jianfeng Gao, et al.
 617 Multimodal foundation models: From specialists to general-purpose assistants. *Foundations and*
 618 *Trends® in Computer Graphics and Vision*, 16(1-2):1–214, 2024b.

619 Junnan Li, Dongxu Li, Caiming Xiong, and Steven Hoi. Blip: Bootstrapping language-image pre-
 620 training for unified vision-language understanding and generation. In *International conference on*
 621 *machine learning*, pp. 12888–12900, 2022.

622

623 Siheng Li, Cheng Yang, Zesen Cheng, Lemao Liu, Mo Yu, Yujiu Yang, and Wai Lam. Large language
 624 models can self-improve in long-context reasoning. *arXiv preprint arXiv:2411.08147*, 2024c.

625 Xianhang Li, Haoqin Tu, Mude Hui, Zeyu Wang, Bingchen Zhao, Junfei Xiao, Sucheng Ren, Jieru
 626 Mei, Qing Liu, Huangjie Zheng, et al. What if we recaption billions of web images with llama-3?
 627 *arXiv preprint arXiv:2406.08478*, 2024d.

628

629 Yifan Li, Yifan Du, Kun Zhou, Jinpeng Wang, Wayne Xin Zhao, and Ji-Rong Wen. Evaluating
 630 object hallucination in large vision-language models. In *Proceedings of the 2023 Conference on*
 631 *Empirical Methods in Natural Language Processing*, pp. 292–305, 2023.

632 Ji Lin, Hongxu Yin, Wei Ping, Pavlo Molchanov, Mohammad Shoeybi, and Song Han. Vila: On
 633 pre-training for visual language models. In *Proceedings of the IEEE/CVF conference on computer*
 634 *vision and pattern recognition*, pp. 26689–26699, 2024.

635

636 Haotian Liu, Chunyuan Li, Qingyang Wu, and Yong Jae Lee. Visual instruction tuning. *Advances in*
 637 *neural information processing systems*, 36:34892–34916, 2023.

638 Haotian Liu, Chunyuan Li, Yuheng Li, and Yong Jae Lee. Improved baselines with visual instruction
 639 tuning. In *Proceedings of the IEEE/CVF Conference on Computer Vision and Pattern Recognition*,
 640 pp. 26296–26306, 2024a.

641 Haotian Liu, Chunyuan Li, Yuheng Li, Bo Li, Yuanhan Zhang, Sheng Shen, and Yong Jae Lee.
 642 Llava-next: Improved reasoning, ocr, and world knowledge. [https://llava-vl.github.](https://llava-vl.github.io/blog/2024-01-30-llava-next/)
 643 [io/blog/2024-01-30-llava-next/](https://llava-vl.github.io/blog/2024-01-30-llava-next/), January 2024b.

644

645 Shilong Liu, Zhaoyang Zeng, Tianhe Ren, Feng Li, Hao Zhang, Jie Yang, Qing Jiang, Chunyuan
 646 Li, Jianwei Yang, Hang Su, et al. Grounding dino: Marrying dino with grounded pre-training
 647 for open-set object detection. In *European Conference on Computer Vision*, pp. 38–55. Springer,
 2024c.

648 Yuan Liu, Haodong Duan, Yuanhan Zhang, Bo Li, Songyang Zhang, Wangbo Zhao, Yike Yuan, Jiaqi
 649 Wang, Conghui He, Ziwei Liu, et al. Mmbench: Is your multi-modal model an all-around player?
 650 In *European conference on computer vision*, pp. 216–233. Springer, 2024d.

651 Yuliang Liu, Zhang Li, Mingxin Huang, Biao Yang, Wenwen Yu, Chunyuan Li, Xu-Cheng Yin,
 652 Cheng-Lin Liu, Lianwen Jin, and Xiang Bai. Ocrbench: on the hidden mystery of ocr in large
 653 multimodal models. *Science China Information Sciences*, 67(12):220102, 2024e.

654 Zichen Liu, Changyu Chen, Wenjun Li, Penghui Qi, Tianyu Pang, Chao Du, Wee Sun Lee, and Min
 655 Lin. Understanding r1-zero-like training: A critical perspective. *arXiv preprint arXiv:2503.20783*,
 656 2025.

657 Haoyu Lu, Wen Liu, Bo Zhang, Bingxuan Wang, Kai Dong, Bo Liu, Jingxiang Sun, Tongzheng Ren,
 658 Zhuoshu Li, Hao Yang, et al. Deepseek-vl: towards real-world vision-language understanding.
 659 *arXiv preprint arXiv:2403.05525*, 2024a.

660 Pan Lu, Swaroop Mishra, Tanglin Xia, Liang Qiu, Kai-Wei Chang, Song-Chun Zhu, Oyvind Tafjord,
 661 Peter Clark, and Ashwin Kalyan. Learn to explain: Multimodal reasoning via thought chains for
 662 science question answering. *Advances in Neural Information Processing Systems*, 35:2507–2521,
 663 2022.

664 Pan Lu, Hritik Bansal, Tony Xia, Jiacheng Liu, Chunyuan Li, Hannaneh Hajishirzi, Hao Cheng,
 665 Kai-Wei Chang, Michel Galley, and Jianfeng Gao. Mathvista: Evaluating mathematical reasoning
 666 of foundation models in visual contexts. In *The Twelfth International Conference on Learning
 667 Representations*, 2024b.

668 Ahmed Masry, Xuan Long Do, Jia Qing Tan, Shafiq Joty, and Enamul Hoque. Chartqa: A benchmark
 669 for question answering about charts with visual and logical reasoning. In *Findings of the Association
 670 for Computational Linguistics: ACL 2022*, pp. 2263–2279, 2022.

671 OpenAI. Gpt-4v(ision) system card. <https://openai.com/index/gpt-4v-system-card/>, 2023.

672 PaddlePaddle Team. Paddleocr. <https://github.com/PaddlePaddle/PaddleOCR>, 2020.

673 Zhiliang Peng, Wenhui Wang, Li Dong, Yaru Hao, Shaohan Huang, Shuming Ma, and Furu
 674 Wei. Kosmos-2: Grounding multimodal large language models to the world. *arXiv preprint
 675 arXiv:2306.14824*, 2023.

676 Alec Radford, Jong Wook Kim, Chris Hallacy, Aditya Ramesh, Gabriel Goh, Sandhini Agarwal,
 677 Girish Sastry, Amanda Askell, Pamela Mishkin, Jack Clark, et al. Learning transferable visual
 678 models from natural language supervision. In *International conference on machine learning*, pp.
 679 8748–8763, 2021.

680 Rafael Rafailov, Archit Sharma, Eric Mitchell, Christopher D Manning, Stefano Ermon, and Chelsea
 681 Finn. Direct preference optimization: Your language model is secretly a reward model. *Advances
 682 in Neural Information Processing Systems*, 36:53728–53741, 2023.

683 Christoph Schuhmann, Romain Beaumont, Richard Vencu, Cade Gordon, Ross Wightman, Mehdi
 684 Cherti, Theo Coombes, Aarush Katta, Clayton Mullis, Mitchell Wortsman, et al. Laion-5b: An
 685 open large-scale dataset for training next generation image-text models. *Advances in neural
 686 information processing systems*, 35:25278–25294, 2022.

687 Shital Shah. Posts on ilya sutskever’s talk at NeurIPS 2024. [https://x.com/sytelus/
 688 status/1857102074070352290](https://x.com/sytelus/status/1857102074070352290), 2024.

689 Piyush Sharma, Nan Ding, Sebastian Goodman, and Radu Soricut. Conceptual captions: A cleaned,
 690 hypernymed, image alt-text dataset for automatic image captioning. In *Proceedings of the 56th
 691 Annual Meeting of the Association for Computational Linguistics (Volume 1: Long Papers)*, pp.
 692 2556–2565, 2018.

693 Min Shi, Fuxiao Liu, Shihao Wang, Shijia Liao, Subhashree Radhakrishnan, Yilin Zhao, De-An
 694 Huang, Hongxu Yin, Karan Sapra, Yaser Yacoob, et al. Eagle: Exploring the design space for
 695 multimodal llms with mixture of encoders. *arXiv preprint arXiv:2408.15998*, 2024.

702 David Silver and Richard S Sutton. Welcome to the era of experience. *Google AI*, 2025.
 703

704 Yanpeng Sun, Jing Hao, Ke Zhu, Jiang-Jiang Liu, Yuxiang Zhao, Xiaofan Li, Gang Zhang, Zechao
 705 Li, and Jingdong Wang. Descriptive caption enhancement with visual specialists for multimodal
 706 perception. *arXiv preprint arXiv:2412.14233*, 2024.

707 Ilya Sutskever. Sequence to sequence learning with neural networks: what a decade, talk at NeurIPS
 708 2024. <https://www.youtube.com/watch?v=1yvBqasHLZs>, November 2024.
 709

710 Teknium. Openhermes 2.5: An open dataset of synthetic data for generalist llm assistants. <https://huggingface.co/datasets/teknium/OpenHermes-2.5>, 2023.
 711

712 Fengwei Teng, Zhaoyang Yu, Quan Shi, Jiayi Zhang, Chenglin Wu, and Yuyu Luo. Atom of thoughts
 713 for markov llm test-time scaling. *arXiv preprint arXiv:2502.12018*, 2025.
 714

715 Rubèn Tito, Dimosthenis Karatzas, and Ernest Valveny. Document collection visual question
 716 answering. In *International Conference on Document Analysis and Recognition*, pp. 778–792.
 717 Springer, 2021.

718

719 Peter Tong, Ellis Brown, Penghao Wu, Sanghyun Woo, Adithya Jairam Vedagiri IYER, Sai Charitha
 720 Akula, Shusheng Yang, Jihan Yang, Manoj Middepogu, Ziteng Wang, et al. Cambrian-1: A fully
 721 open, vision-centric exploration of multimodal llms. *Advances in Neural Information Processing
 722 Systems*, 37:87310–87356, 2024.

723 Peng Wang, Shuai Bai, Sinan Tan, Shijie Wang, Zhihao Fan, Jinze Bai, Keqin Chen, Xuejing Liu,
 724 Jialin Wang, Wenbin Ge, et al. Qwen2-vl: Enhancing vision-language model’s perception of the
 725 world at any resolution. *arXiv preprint arXiv:2409.12191*, 2024.

726

727 Xuezhi Wang, Jason Wei, Dale Schuurmans, Quoc Le, Ed Chi, Sharan Narang, Aakanksha Chowdh-
 728 ery, and Denny Zhou. Self-consistency improves chain of thought reasoning in language models.
 729 *arXiv preprint arXiv:2203.11171*, 2022.

730

731 Jason Wei and Hyung Won Chung. Stanford cs25: V4. <https://www.youtube.com/watch?v=3gb-ZkVRemQ&t=3933s>, 2024.
 732

733 Jason Wei, Xuezhi Wang, Dale Schuurmans, Maarten Bosma, Fei Xia, Ed Chi, Quoc V Le, Denny
 734 Zhou, et al. Chain-of-thought prompting elicits reasoning in large language models. *Advances in
 735 neural information processing systems*, 35:24824–24837, 2022.

736

737 Ian Wu, Patrick Fernandes, Amanda Bertsch, Seungone Kim, Sina Pakazad, and Graham Neubig.
 738 Better instruction-following through minimum bayes risk. *arXiv preprint arXiv:2410.02902*, 2024.

739

740 X.AI. Grok-1.5 vision preview. <https://x.ai/blog/grok-1.5v>, 2024.

741

742 Kun Xiang, Zhili Liu, Zihao Jiang, Yunshuang Nie, Runhui Huang, Haoxiang Fan, Hanhui Li, Weiran
 743 Huang, Yihan Zeng, Jianhua Han, et al. Atomthink: A slow thinking framework for multimodal
 744 mathematical reasoning. *arXiv preprint arXiv:2411.11930*, 2024.

745

746 Guowei Xu, Peng Jin, Hao Li, Yibing Song, Lichao Sun, and Li Yuan. Llava-cot: Let vision language
 747 models reason step-by-step. *arXiv preprint arXiv:2411.10440*, 2025.

748

749 Xiao Xu, Tianhao Niu, Yuxi Xie, Libo Qin, Wanxiang Che, and Min-Yen Kan. Exploring
 750 multi-grained concept annotations for multimodal large language models. *arXiv preprint
 751 arXiv:2412.05939*, 2024a.

752

753 Zhiyang Xu, Chao Feng, Rulin Shao, Trevor Ashby, Ying Shen, Di Jin, Yu Cheng, Qifan Wang, and
 754 Lifu Huang. Vision-flan: Scaling human-labeled tasks in visual instruction tuning. In *Findings of
 755 the Association for Computational Linguistics ACL 2024*, pp. 15271–15342, 2024b.

756

757 Le Xue, Manli Shu, Anas Awadalla, Jun Wang, An Yan, Senthil Purushwalkam, Honglu Zhou, Viraj
 758 Prabhu, Yutong Dai, Michael S Ryoo, et al. xgen-mm (blip-3): A family of open large multimodal
 759 models. *arXiv preprint arXiv:2408.08872*, 2024.

756 An Yang, Baosong Yang, Binyuan Hui, Bo Zheng, Bowen Yu, Chang Zhou, Chengpeng Li,
 757 Chengyuan Li, Dayiheng Liu, Fei Huang, et al. Qwen2 technical report. *arXiv preprint*
 758 *arXiv:2407.10671*, 2024a.

759 An Yang, Baosong Yang, Beichen Zhang, Binyuan Hui, Bo Zheng, Bowen Yu, Chengyuan Li,
 760 Dayiheng Liu, Fei Huang, Haoran Wei, et al. Qwen2. 5 technical report. *arXiv preprint*
 761 *arXiv:2412.15115*, 2024b.

762 Jiabo Ye, Anwen Hu, Haiyang Xu, Qinghao Ye, Ming Yan, Guohai Xu, Chenliang Li, Junfeng Tian,
 763 Qi Qian, Ji Zhang, et al. Ureader: Universal ocr-free visually-situated language understanding with
 764 multimodal large language model. In *Findings of the Association for Computational Linguistics: EMNLP 2023*, pp. 2841–2858, 2023.

765 Shukang Yin, Chaoyou Fu, Sirui Zhao, Ke Li, Xing Sun, Tong Xu, and Enhong Chen. A survey on
 766 multimodal large language models. *National Science Review*, 11(12), 2024.

767 Qiying Yu, Quan Sun, Xiaosong Zhang, Yufeng Cui, Fan Zhang, Yue Cao, Xinlong Wang, and
 768 Jingjing Liu. Capsfusion: Rethinking image-text data at scale. In *Proceedings of the IEEE/CVF Conference on Computer Vision and Pattern Recognition*, pp. 14022–14032, 2024a.

769 Weihao Yu, Zhengyuan Yang, Linjie Li, Jianfeng Wang, Kevin Lin, Zicheng Liu, Xinchao Wang,
 770 and Lijuan Wang. Mm-vet: evaluating large multimodal models for integrated capabilities. In *Proceedings of the 41st International Conference on Machine Learning*, pp. 57730–57754, 2024b.

771 Xiang Yue, Yuansheng Ni, Kai Zhang, Tianyu Zheng, Ruqi Liu, Ge Zhang, Samuel Stevens, Dongfu
 772 Jiang, Weiming Ren, Yuxuan Sun, et al. Mmmu: A massive multi-discipline multimodal understanding and reasoning benchmark for expert agi. In *Proceedings of the IEEE/CVF Conference on Computer Vision and Pattern Recognition*, pp. 9556–9567, 2024a.

773 Xiang Yue, Yuansheng Ni, Kai Zhang, Tianyu Zheng, Ruqi Liu, Ge Zhang, Samuel Stevens, Dongfu
 774 Jiang, Weiming Ren, Yuxuan Sun, et al. Mmmu: A massive multi-discipline multimodal understanding and reasoning benchmark for expert agi. In *Proceedings of the IEEE/CVF Conference on Computer Vision and Pattern Recognition*, pp. 9556–9567, 2024b.

775 Xiaoying Zhang, Baolin Peng, Ye Tian, Jingyan Zhou, Lifeng Jin, Linfeng Song, Haitao Mi, and
 776 Helen Meng. Self-alignment for factuality: Mitigating hallucinations in llms via self-evaluation. In *Proceedings of the 62nd Annual Meeting of the Association for Computational Linguistics (Volume 1: Long Papers)*, pp. 1946–1965, 2024a.

777 Yipeng Zhang, Yifan Liu, Zonghao Guo, Yidan Zhang, Xuesong Yang, Chi Chen, Jun Song, Bo Zheng,
 778 Yuan Yao, Zhiyuan Liu, et al. Llava-uhd v2: an mllm integrating high-resolution feature pyramid via
 779 hierarchical window transformer. *arXiv preprint arXiv:2412.13871*, 2024b.

780 Zhuosheng Zhang, Aston Zhang, Mu Li, and Alex Smola. Automatic chain of thought prompting in
 781 large language models. In *The Eleventh International Conference on Learning Representations*, 2023.

782 Zhuosheng Zhang, Aston Zhang, Mu Li, George Karypis, Alex Smola, et al. Multimodal chain-of-thought reasoning in language models. *Transactions on Machine Learning Research*, 2024c.

783 Baining Zhao, Ziyu Wang, Jianjie Fang, Chen Gao, Fanhang Man, Jinqiang Cui, Xin Wang,
 784 Xinlei Chen, Yong Li, and Wenwu Zhu. Embodied-r: Collaborative framework for activating
 785 embodied spatial reasoning in foundation models via reinforcement learning. *arXiv preprint*
 786 *arXiv:2504.12680*, 2025.

787

788

789

790

791

792

793

794

795

796

797

798

799

800

801

802

803

804

805

806

807

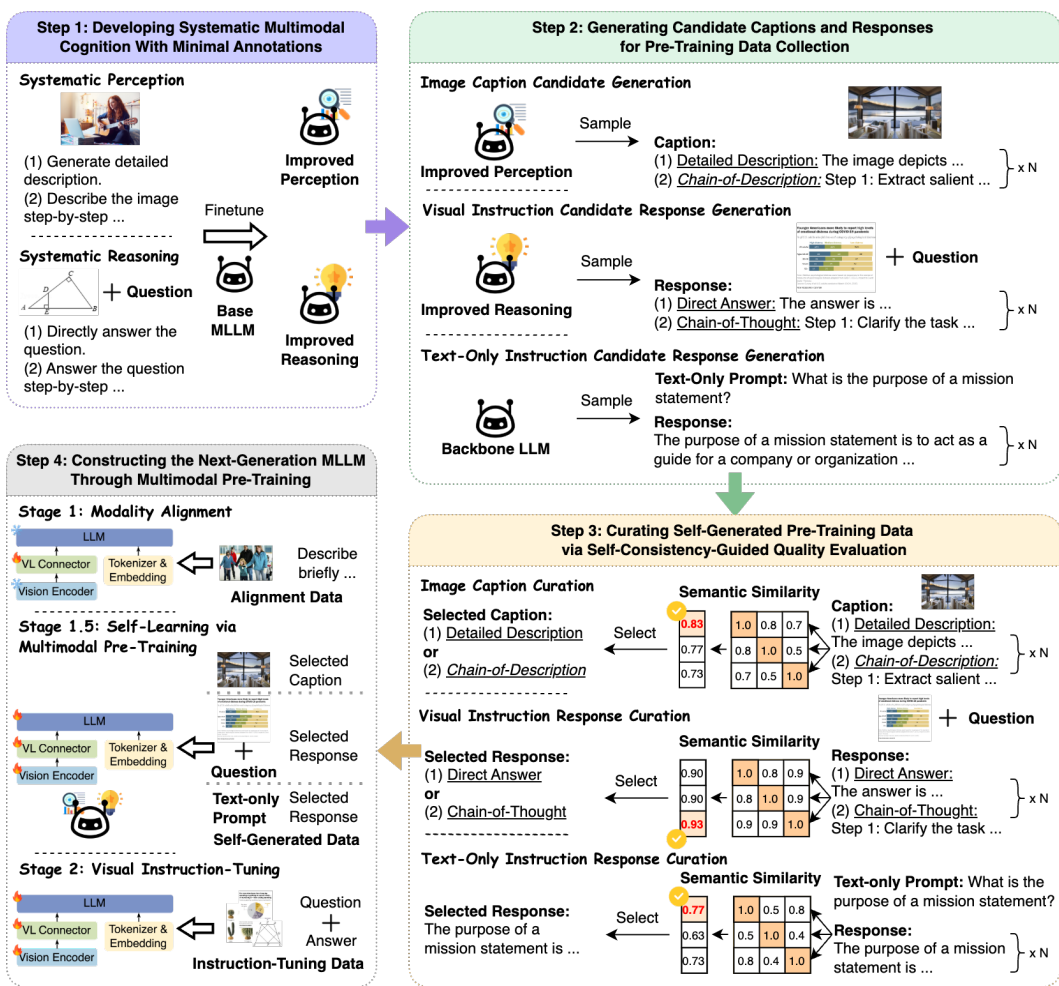
808

809

| | | |
|-----|---|-----------|
| 810 | CONTENTS | |
| 811 | | |
| 812 | | |
| 813 | A The Use of Large Language Models (LLMs) | 18 |
| 814 | | |
| 815 | B The Comprehensive Illustration of SICOG | 19 |
| 816 | B.1 Enhancing Systematic perception with <i>Chain-of-Description</i> | 23 |
| 817 | B.2 Improving Systematic Reasoning with Structured Chain-of-Thought | 24 |
| 818 | | |
| 819 | | |
| 820 | C Mathematical Proof of SICOG | 26 |
| 821 | C.1 Definitions | 26 |
| 822 | C.2 The Iterative Cycle | 26 |
| 823 | C.3 Core Assumptions | 26 |
| 824 | C.4 The Proof of Non-Decreasing Capability | 27 |
| 825 | | |
| 826 | | |
| 827 | | |
| 828 | D Detailed Discussion on Related Work | 28 |
| 829 | | |
| 830 | | |
| 831 | E Can Preference Learning Support SICOG’s Systematic Perception and Reasoning De- | 29 |
| 832 | velopment? | |
| 833 | | |
| 834 | F How Does SICOG Enhance the Reasoning Capabilities of Foundation MLLMs? | 30 |
| 835 | | |
| 836 | G How Does Scaling Self-Generated Pre-Training Data Affect the Performance of SICOG? | 32 |
| 837 | | |
| 838 | | |
| 839 | H Does SICOG Remain Effective When Varying Recaptioned Images? | 32 |
| 840 | | |
| 841 | I Can SICOG Contribute to the Construction of Next-Generation Foundation MLLMs | 34 |
| 842 | through Continuous Cognitive Self-Improvement? | |
| 843 | | |
| 844 | J How Do <i>Chain-of-Description</i> and <i>Chain-of-Thought</i> Improve Cognition? | 35 |
| 845 | | |
| 846 | J.1 How Does <i>Chain-of-Description</i> Facilitate Multimodal Perception? | 35 |
| 847 | J.2 How Does Structured Chain-of-Thought Enhance Multimodal Reasoning? | 36 |
| 848 | | |
| 849 | | |
| 850 | K Fine-Grained Evaluation across Six Core Capabilities | 38 |
| 851 | | |
| 852 | L Distribution of Generated Caption Token Lengths | 38 |
| 853 | | |
| 854 | M Implementation Details | 39 |
| 855 | | |
| 856 | M.1 Compared Methods. | 39 |
| 857 | M.2 Implementation Details. | 40 |
| 858 | | |
| 859 | M.3 Implementation Details of Compared Methods. | 41 |
| 860 | | |
| 861 | N Analysis of Computational Cost | 43 |
| 862 | | |
| 863 | O Mitigating Potential Performance Saturation and Error Propagation | 44 |

| | | |
|-----|--|-----------|
| 864 | P Additional Experimental Results | 45 |
| 865 | | |
| 866 | Q Prompts | 46 |
| 867 | | |
| 868 | R Training Examples | 48 |
| 869 | | |
| 870 | S Limitations | 51 |
| 871 | | |
| 872 | | |
| 873 | | |
| 874 | | |
| 875 | | |
| 876 | | |
| 877 | | |
| 878 | | |
| 879 | | |
| 880 | | |
| 881 | | |
| 882 | | |
| 883 | | |
| 884 | | |
| 885 | | |
| 886 | | |
| 887 | | |
| 888 | | |
| 889 | | |
| 890 | | |
| 891 | | |
| 892 | | |
| 893 | | |
| 894 | | |
| 895 | | |
| 896 | | |
| 897 | | |
| 898 | | |
| 899 | | |
| 900 | | |
| 901 | | |
| 902 | | |
| 903 | | |
| 904 | | |
| 905 | | |
| 906 | | |
| 907 | | |
| 908 | | |
| 909 | | |
| 910 | | |
| 911 | | |
| 912 | | |
| 913 | | |
| 914 | | |
| 915 | | |
| 916 | | |
| 917 | | |

918 **A THE USE OF LARGE LANGUAGE MODELS (LLMs)**
919920 In this paper, we utilized LLMs, specifically GPT-4o (Hurst et al., 2024), for two limited purposes:
921 (1) to evaluate the quality of generated captions using our specially designed rubrics (detailed in
922 Appendix J); and (2) to assist in refining the manuscript’s language for clarity and fluency. LLMs
923 were not involved in research ideation, experimental design, or drafting the initial version of the
924 paper.925
926
927
928
929
930
931
932
933
934
935
936
937
938
939
940
941
942
943
944
945
946
947
948
949
950
951
952
953
954
955
956
957
958
959
960
961
962
963
964
965
966
967
968
969
970
971

972 B THE COMPREHENSIVE ILLUSTRATION OF SICOG
973
974

1006 Figure 3: The SICOG framework consists of four steps: (i) **Enhancing multimodal cognition**: Fine-
1007 tune an MLLM using minimal annotated data—the *Chain-of-Description* format and visual instruction-tuning data with structured CoT—to improve systematic perception
1008 and reasoning (upper left). (ii) **Generating candidate data**: Use the improved models to sample
1009 candidate captions and responses for pre-training (upper right). (iii) **Curating pre-training data**:
1010 Apply self-consistency-guided quality evaluation to select the most semantically consistent, self-
1011 generated candidates for learning (lower right). (iv) **Constructing the next-generation MLLM**:
1012 Perform multimodal pre-training on the curated data to build a foundation MLLM with enhanced
1013 self-improving cognition (lower left).

1015 The goal of SICOG is to advance MLLMs by equipping them with rich multimodal knowledge and
1016 systematic cognitive capabilities—namely, systematic visual understanding (“how to observe”) and
1017 in-depth multimodal reasoning (“how to think”)—during multimodal pre-training, with minimal
1018 reliance on external annotations. As illustrated in Figure 2, SICOG operates through four key steps.
1019

1020 **Step 1: Developing systematic multimodal cognitive capabilities with minimal annotated data.**
1021 We first equip a given MLLM \mathcal{M} , parameterized by θ , with systematic perception and reasoning
1022 abilities while using *minimal* annotated multimodal data. This involves fine-tuning the model to
1023 develop structured, multi-step perception and reasoning chains, enabling it to systematically process
1024 and integrate multimodal information.

1025 Specifically, this step consists of the following two core components:

1026
 1027
 1028
 1029
 1030
 1031
 1032

- **Systematic multimodal perception.** To enhance the MLLM’s ability to systematically observe and interpret images, we fine-tune \mathcal{M} using a combination of image-captioning datasets, yielding a model with improved perception, $\mathcal{M}_0^{\text{Perception}}$. Specifically, these datasets consist of images v , prompts x , intermediate step-by-step analyses s , and descriptions y , structured in two formats of captions: Detailed Description (DD) and *Chain-of-Description* (CoD) (see Section 3.2 for details on the *Chain-of-Description* strategy and data collection.)

1033
$$\mathcal{D}^{\text{Perception}} = \mathcal{D}_{DD}^{\text{Perception}} + \mathcal{D}_{CoD}^{\text{Perception}} = \{(v_i, x_i, y_i)\}_{i=1}^N + \{(v_i, x_i, s_i, y_i)\}_{i=1}^N, \quad (6)$$

1034 where N is the number of samples in each dataset. The model is fine-tuned using the
 1035 following objective, improving its multimodal perception:

1036
$$\mathcal{M}_0^{\text{Perception}} \leftarrow \mathcal{J}_\theta(\mathcal{D}^{\text{Perception}}) = \sum_{i=1}^N [\log p_\theta(y | v, x) + \log p_\theta(s, y | v, x)] \quad (7)$$

1037
 1038
 1039

- **Systematic multimodal reasoning.** Similarly, to strengthen the model’s systematic and in-depth reasoning capabilities, we fine-tune \mathcal{M} using a mix of visual instruction-tuning datasets, yielding a model with enhanced reasoning, $\mathcal{M}_0^{\text{Reasoning}}$. These datasets consist of images v , questions q , intermediate step-by-step rationales r , and answers a , structured in two formats of responses: *Direct Answer* (DA) and *Chain-of-Thought* (CoT) (see Section 3.3 for details on data curation).

1040
$$\mathcal{D}^{\text{Reasoning}} = \mathcal{D}_{DA}^{\text{Reasoning}} + \mathcal{D}_{CoT}^{\text{Reasoning}} = \{(v_i, q_i, a_i)\}_{i=1}^M + \{(v_i, q_i, r_i, a_i)\}_{i=1}^M, \quad (8)$$

1041 where M is the number of samples in each dataset. The model is fine-tuned using the
 1042 following objective, fostering its multimodal reasoning:

1043
$$\mathcal{M}_0^{\text{Reasoning}} \leftarrow \mathcal{J}_\theta(\mathcal{D}^{\text{Reasoning}}) = \sum_{i=1}^M [\log p_\theta(a | v, q) + \log p_\theta(r, a | v, q)] \quad (9)$$

1044
 1045
 1046
 1047
 1048
 1049
 1050
 1051
 1052
 1053
 1054
 1055
 1056
 1057
 1058
 1059
 1060
 1061
 1062
 1063
 1064
 1065
 1066
 1067
 1068
 1069
 1070
 1071
 1072
 1073
 1074
 1075
 1076
 1077
 1078
 1079

Step 2: Generating candidate captions and responses for pre-training data collection. Next, we construct multimodal pre-training data by leveraging the improved models, $\mathcal{M}_0^{\text{Perception}}$ and $\mathcal{M}_0^{\text{Reasoning}}$, to generate candidate image captions and visual instruction responses. Additionally, to mitigate potential degradation of the MLLM’s language capabilities during multimodal pre-training, we prompt the backbone large language model (LLM), \mathcal{M}_{LLM} , to generate candidate responses for text-only instructions.

This step consists of three key components:

- **Image caption candidate generation.** Given a collection of unlabeled images $\{v_k\}_{k=1}^K$, we prompt $\mathcal{M}_0^{\text{Perception}}$ (with policy $p_{\mathcal{M}_0^{\text{Perception}}}$) using two types of prompts to generate detailed descriptions and induce *Chain-of-Description* perception:
 1. “Please generate a detailed caption of this image. Be as descriptive as possible.” (x_{DD}).
 2. “Please generate a detailed caption of this image. Describe the image step by step.” (x_{CoD}).

Specifically, for a given image v_k , the model $\mathcal{M}_0^{\text{Perception}}$ generates multiple candidate captions via sampling:

$$\begin{aligned} \{\hat{y}_k\} &\sim p_{\mathcal{M}_0^{\text{Perception}}}(\cdot | v_k, x_{DD}), \\ \{(\hat{s}_k, \hat{y}_k)\} &\sim p_{\mathcal{M}_0^{\text{Perception}}}(\cdot | v_k, x_{CoD}), \end{aligned} \quad (10)$$

where $\{\hat{y}_k\}$ represents the set of detailed descriptions, and $\{(\hat{s}_k, \hat{y}_k)\}$ represents the set of step-by-step analyses along with corresponding detailed descriptions. This results in a collection of candidate image captions in two formats:

$$\mathcal{D}_{\text{Cand}}^{\text{Perception}} = \{(v_k, x_{DD}, \{\hat{y}_k\})\}_{k=1}^K + \{(v_k, x_{CoD}, \{(\hat{s}_k, \hat{y}_k)\})\}_{k=1}^K. \quad (11)$$

1080
 1081 • **Visual instruction candidate response generation.** Similarly, given a collection of un-
 1082 labeled images $\{v_z\}_{z=1}^Z$ with corresponding questions q_z , we prompt $\mathcal{M}_0^{\text{Reasoning}}$ (with
 1083 policy $p_{\mathcal{M}_0^{\text{Reasoning}}}$) using two types of prompts to generate direct answers (DA) and induce
 1084 *Chain-of-Thought* (CoT) reasoning:
 1085 1. "<original question>." (q_{DA}).
 1086 2. "<original question> Answer the question step by step."
 1087 (q_{CoT}).

1088 Specifically, for a given image v_z and corresponding question q_z , the model $\mathcal{M}_0^{\text{Reasoning}}$
 1089 generates multiple candidate responses:

$$1090 \begin{aligned} \{\hat{a}_z\} &\sim p_{\mathcal{M}_0^{\text{Reasoning}}}(\cdot | v_z, q_{DA}), \\ 1091 \{(\hat{r}_z, \hat{a}_z)\} &\sim p_{\mathcal{M}_0^{\text{Reasoning}}}(\cdot | v_z, q_{CoT}), \end{aligned} \quad (12)$$

1093 where $\{\hat{a}_z\}$ represents the set of direct answers, and $\{(\hat{r}_z, \hat{a}_z)\}$ represents the set of step-by-
 1094 step rationales along with corresponding answers. This results in a collection of candidate
 1095 visual instruction responses in two formats:

$$1096 \mathcal{D}_{\text{Cand}}^{\text{Reasoning}} = \{(v_z, q_{DA}, \{\hat{a}_z\})\}_{z=1}^Z + \{(v_z, q_{CoT}, \{(\hat{r}_z, \hat{a}_z)\})\}_{z=1}^Z. \quad (13)$$

1097 • **Text-only instruction candidate response generation.** To maintain language capabilities,
 1098 we generate textual instruction responses using the backbone LLM, \mathcal{M}_{LLM} (with policy
 1099 $p_{\mathcal{M}_{LLM}}$), based on a collection of unlabeled text prompts $\{x_t\}_{t=1}^T$.

1100 Specifically, for a given prompt x_t , the model \mathcal{M}_{LLM} generates a set of candidate responses:

$$1101 \{\hat{y}_t\} \sim p_{\mathcal{M}_{LLM}}(\cdot | x_t), \quad (14)$$

1102 resulting in a collection of candidate textual instruction responses:

$$1103 \mathcal{D}_{\text{Cand}}^{\text{Language}} = \{(x_t, \{\hat{y}_t\})\}_{t=1}^T. \quad (15)$$

1105 Step 3: Curating self-generated pre-training data via self-consistency-guided quality evaluation.

1106 To ensure the quality of self-generated pre-training data, we employ *self-consistency* to evaluate
 1107 candidate samples without external supervision. This method is based on the principle that higher-
 1108 quality candidates exhibit greater semantic consistency (Wu et al., 2024). The most consistent
 1109 candidates are selected for further self-refinement during multimodal pre-training.

1110 Specifically, we apply a semantic-similarity-guided self-consistency evaluation function, $f(\cdot)$. For
 1111 each instance (e.g., an unlabeled image), it assesses the quality of candidates (e.g., candidate captions)
 1112 by comparing each candidate against all others based on semantic similarity and selects the candidate
 1113 with the highest consistency score, provided it exceeds a predefined threshold τ (i.e., otherwise, the
 1114 instance and its candidates are skipped):

$$1116 f(\{c\}) = \arg \max_{c \in \{c\}} \frac{1}{N_{\text{cand}}} \sum_{j=1}^{N_{\text{cand}}} \text{sim}(c, c^{(j)}), \quad \text{s.t.} \quad \max_{c \in \{c\}} \frac{1}{N_{\text{cand}}} \sum_{j=1}^{N_{\text{cand}}} \text{sim}(c, c^{(j)}) \geq \tau, \quad (16)$$

1120 where N_{cand} is the number of candidate samples being compared, and $\{c\}$ is the candidate set.

1121 We apply this method as follows:

1123 • **Self-generated image caption curation.** For each image v_k , we apply $f(\cdot)$ to assess the
 1124 quality of candidate captions by comparing each generated description in the caption against
 1125 all others. The most consistent caption is selected as the final self-generated caption:

$$1126 \begin{aligned} \hat{y}_{\text{selected}} \vee (\hat{s}_{\text{selected}}, \hat{y}_{\text{selected}}) &= f(\{\hat{y}_k\} \cup \{(\hat{s}_k, \hat{y}_k)\}) \\ 1127 &= \arg \max_{y \in \{\hat{y}_k\} \cup \{(\hat{s}_k, \hat{y}_k)\}} \frac{1}{N_{\text{cand}}} \sum_{j=1}^{N_{\text{cand}}} \text{sim}(y, y^{(j)}), \\ 1128 &\quad \text{s.t.} \quad \max_{y \in \{\hat{y}_k\} \cup \{(\hat{s}_k, \hat{y}_k)\}} \frac{1}{N_{\text{cand}}} \sum_{j=1}^{N_{\text{cand}}} \text{sim}(y, y^{(j)}) \geq \tau^{\text{Perception}}. \end{aligned} \quad (17)$$

1134 where $N_{\text{cand}} = |\{\hat{y}_k\} \cup \{(\hat{s}_k, \hat{y}_k)\}|$ is the total number of candidate captions for each image.
 1135 The curated dataset of self-generated image captions is:
 1136

$$\mathcal{D}_{\text{Selected}}^{\text{Perception}} = \{(v, x_{DD}, \hat{y}_{\text{selected}}) \vee (v, x_{CoD}, \hat{s}_{\text{selected}}, \hat{y}_{\text{selected}})\}_{k=1}^K. \quad (18)$$

- **Self-generated visual instruction response curation.** Similarly, for each image v_z and corresponding question q_z , we apply $f(\cdot)$ to evaluate candidate responses, selecting the most consistent response:

$$\begin{aligned} \hat{a}_{\text{selected}} \vee (\hat{r}_{\text{selected}}, \hat{a}_{\text{selected}}) &= f(\{\hat{a}_z\} \cup \{(\hat{r}_z, \hat{a}_z)\}) \\ &= \arg \max_{a \in \{\hat{a}_z\} \cup \{(\hat{r}_z, \hat{a}_z)\}} \frac{1}{N_{\text{cand}}} \sum_{j=1}^{N_{\text{cand}}} \text{sim}(a, a^{(j)}), \\ \text{s.t. } & \max_{a \in \{\hat{a}_z\} \cup \{(\hat{r}_z, \hat{a}_z)\}} \frac{1}{N_{\text{cand}}} \sum_{j=1}^{N_{\text{cand}}} \text{sim}(a, a^{(j)}) \geq \tau^{\text{Reasoning}}. \end{aligned} \quad (19)$$

1151 where $N_{\text{cand}} = |\{\hat{a}_z\} \cup \{(\hat{r}_z, \hat{a}_z)\}|$ is the total number of candidate responses for each
 1152 question. The curated set of self-generated visual instruction responses is:
 1153

$$\mathcal{D}_{\text{Selected}}^{\text{Reasoning}} = \{(v_z, q_{DA}, \hat{a}_{\text{selected}}) \vee (v_z, q_{CoT}, \hat{r}_{\text{selected}}, \hat{a}_{\text{selected}})\}_{z=1}^Z. \quad (20)$$

- **Self-generated text-only instruction response curation.** Similarly, for each prompt x_t , we apply $f(\cdot)$ to evaluate candidate responses, selecting the most consistent response:

$$\begin{aligned} \hat{y}_{t-\text{selected}} &= f(\{\hat{y}_t\}) \\ &= \arg \max_{y_t \in \{\hat{y}_t\}} \frac{1}{N_{\text{cand}}} \sum_{j=1}^{N_{\text{cand}}} \text{sim}(y_t, y_t^{(j)}) \\ \text{s.t. } & \max_{y_t \in \{\hat{y}_t\}} \frac{1}{N_{\text{cand}}} \sum_{j=1}^{N_{\text{cand}}} \text{sim}(y_t, y_t^{(j)}) \geq \tau^{\text{Language}}. \end{aligned} \quad (21)$$

1166 where $N_{\text{cand}} = |\{\hat{y}_t\}|$ is the total number of candidate responses for each question. The
 1167 curated set of self-generated textual instruction responses is:
 1168

$$\mathcal{D}_{\text{Selected}}^{\text{Language}} = \{(x_t, \hat{y}_{t-\text{selected}})\}_{t=1}^T. \quad (22)$$

1171 Finally, we obtain the curated self-generated multimodal pre-training dataset:
 1172

$$\mathcal{D}^{\text{Pre-training}} = \mathcal{D}_{\text{Selected}}^{\text{Perception}} + \mathcal{D}_{\text{Selected}}^{\text{Reasoning}} + \mathcal{D}_{\text{Selected}}^{\text{Language}}. \quad (23)$$

1175 **Step 4: Constructing the next-generation MLLM through multimodal pre-training.** To build
 1176 the next-generation foundation MLLM, we introduce an intermediate multimodal pre-training stage,
 1177 Stage 1.5, within the standard two-stage training strategy, following Liu et al. (2024b); Li et al.
 1178 (2024a). This stage refines the MLLM using curated self-generated pre-training data. The complete
 1179 training strategy consists of three stages, as shown in the lower left part in Figure 2:
 1180

- **Stage 1: Modality alignment.** In this stage, image features are aligned with the text embedding space. Following Li et al. (2024a), we train only the vision-language (VL) connector using image-text pairs from $\mathcal{D}^{\text{Alignment}}$, while keeping the vision encoder (e.g., vision transformer) and large language model (LLM) frozen.
- **Stage 1.5: Self-learning via multimodal pre-training.** The model undergoes training with curated self-generated pre-training data $\mathcal{D}^{\text{Pre-Training}}$ to acquire multimodal knowledge from these self-generated samples and internalize its systematic multimodal perception and reasoning abilities. During this stage, all model components are fully trainable.

1188
 1189
 1190
 1191

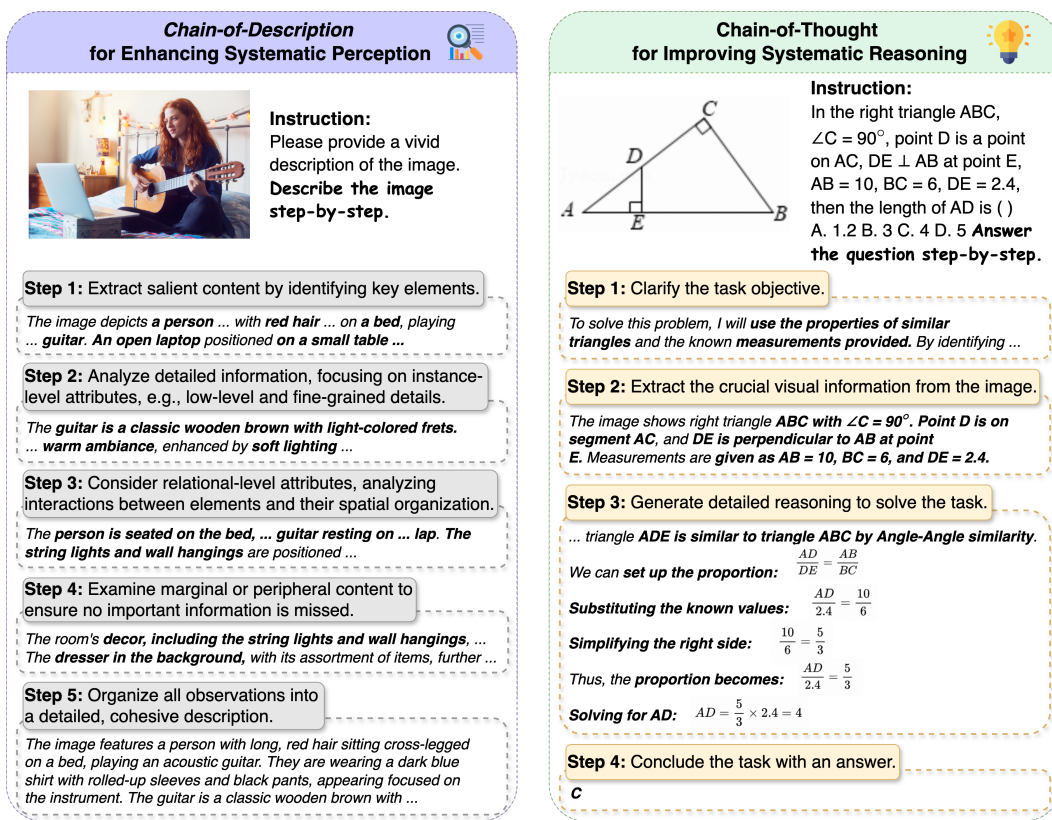
- **Stage 2: Visual instruction-tuning.** In the final stage, the model is fine-tuned using instruction-tuning data $\mathcal{D}^{\text{Instruction-Tuning}}$ to develop robust visual instruction-following capabilities, with all model components fully trainable.

1192 This three-stage training process is formulated as follows, resulting in the next-generation foundation
 1193 MLLM with self-improved cognition $\mathcal{M}^{\text{Next}}$:

1194

$$\begin{aligned} \mathcal{M}^1 &\leftarrow \mathcal{L}_{\phi}^{\text{Stage 1}}(\mathcal{D}^{\text{Alignment}}) \\ \mathcal{M}^{1.5} &\leftarrow \mathcal{L}_{\phi}^{\text{Stage 1.5}}(\mathcal{D}^{\text{Pre-training}}) \\ \mathcal{M}^{\text{Next}} &\leftarrow \mathcal{L}_{\phi}^{\text{Stage 2}}(\mathcal{D}^{\text{Instruction-Tuning}}). \end{aligned} \quad (24)$$

1200
 1201 **B.1 ENHANCING SYSTEMATIC PERCEPTION WITH *Chain-of-Description***
 1202



1229
 1230 **Figure 4: Illustration of *Chain-of-Description* (left) for enhancing systematic perception and struc-
 1231 tured Chain-of-Thought (right) for strengthening reasoning capabilities.**

1232 We introduce *Chain-of-Description* (CoD) to enable systematic and comprehensive perception,
 1233 equipping the MLLM with the ability to logically analyze and describe visual information step by
 1234 step (“how to observe”). This structured approach enhances the MLLM’s efficiency in thoroughly
 1235 interpreting visual content. Specifically, *Chain-of-Description* perception is organized into the
 1236 following five steps (Figure 4, left):

1237

- **Step 1: Extract salient content.** Identify the key elements that define the overall context
 1238 and meaning of the image, laying the foundation for basic visual recognition.
- **Step 2: Analyze detailed information.** Focus on instance-level attributes, such as low-level
 1239 and fine-grained details, *e.g.*, “the guitar is a classic wooden brown with light-colored frets.”
 1240 This step ensures a precise and detailed interpretation of the image.

- 1242 • **Step 3: Consider relational-level attributes.** Analyze interactions between elements and
1243 their spatial organization, *e.g.*, “the person is seated on the bed,” leading to a richer and
1244 more comprehensive understanding of visual relationships.
- 1245 • **Step 4: Examine marginal or peripheral content.** Pay attention to less prominent or
1246 background details, *e.g.*, “the dresser in the background,” to ensure no important information
1247 is overlooked.
- 1248 • **Step 5: Organize all observations.** Synthesize all findings into a cohesive, detailed
1249 description, enabling comprehensive coverage and holistic image understanding.

1251 **Data preparation.** To enable systematic perception in MLLMs, we utilize GPT-4o (Hurst et al.,
1252 2024) with manually curated prompts (Table 20) to generate detailed, step-by-step analyses of visual
1253 features. Specifically, we prompt GPT-4o to recaption 35k images from the Vision-Flan dataset (Xu
1254 et al., 2024b), which provides diverse visual content. A detailed example is presented in Table 22.

1256 B.2 IMPROVING SYSTEMATIC REASONING WITH STRUCTURED CHAIN-OF-THOUGHT

1258 We adopt a structured Chain-of-Thought (CoT) approach (Xu et al., 2025) to enhance systematic
1259 and in-depth reasoning. For completeness, we briefly summarize this approach. It enables the
1260 MLLM to decompose problem-solving into logical steps: analyzing multimodal questions, gathering
1261 relevant visual information, and answering progressively. Specifically, the structured CoT process
1262 (Figure 4, right) follows four logical steps: (i) **Step 1: Clarify the task objective.** Identify the
1263 problem’s requirements and constraints, establishing a foundational understanding. (ii) **Step 2:**
1264 **Extract crucial visual information.** Identify and extract relevant visual elements to enhance
1265 multimodal comprehension. (iii) **Step 3: Generate detailed reasoning.** Construct a logical sequence
1266 of intermediate steps based on the extracted information to derive an answer systematically. (iv)
1267 **Step 4: Conclude with an answer.** Synthesize the reasoning steps into a coherent and accurate final
1268 response.

1269 **Data preparation.** To enable systematic reasoning in the MLLM, we revise the dataset curated
1270 by (Xu et al., 2025). Specifically, we randomly select 35k training examples from LLaVA-CoT, cov-
1271 ering ten well-studied QA tasks, and replace the special tags (*e.g.*, <SUMMARY> and </SUMMARY>)
1272 with curated step-by-step instructions. A detailed example is shown in Table 23.

1273 The complete training process is summarized in Algorithm 1, with implementation details in Sec-
1274 tion 4.1 and Appendix M.

1275
1276
1277
1278
1279
1280
1281
1282
1283
1284
1285
1286
1287
1288
1289
1290
1291
1292
1293
1294
1295

1296

1297

1298

Algorithm 1 SICOG: A Self-Learning Framework for Systematic Multimodal Cognition

1299

- 1: **Input:** Pretrained MLLM \mathcal{M} , parameterized by θ
- 2: Systematic perception data: $\mathcal{D}^{\text{Perception}} = \mathcal{D}_{DD}^{\text{Perception}} + \mathcal{D}_{CoD}^{\text{Perception}}$
- 3: Systematic reasoning data: $\mathcal{D}^{\text{Reasoning}} = \mathcal{D}_{DA}^{\text{Reasoning}} + \mathcal{D}_{CoT}^{\text{Reasoning}}$
- 4: Default alignment data: $\mathcal{D}^{\text{Alignment}}$, instruction-tuning data: $\mathcal{D}^{\text{Instruction-Tuning}}$
- 5: Unlabeled data: (1) unlabeled image sets $\{v_k\}$ with prompts x , (2) unlabeled image sets $\{v_z\}$ with questions q , (3) unlabeled text-only prompts x_t
- 6: **Goal:** Enable systematic visual understanding and reasoning via self-learning
- 7: $\mathcal{M}_0 \leftarrow \mathcal{M}$ # Initialize model
- 8: **for** $n = 1, \dots, N$ **do** # Iterative foundation MLLM update, when applicable
- 9: **Step 1: Systematic Multimodal Cognitive Training**
- 10: Fine-tune perception, reasoning models:

$$\mathcal{M}_{n-1}^{\text{Perception}} \leftarrow \mathcal{J}_\theta(\mathcal{D}^{\text{Perception}}), \mathcal{M}_{n-1}^{\text{Reasoning}} \leftarrow \mathcal{J}_\theta(\mathcal{D}^{\text{Reasoning}})$$

1310

1311

Step 2: Generating Candidate Captions and Responses

1312

- 12: Generate image captions: # Foster multimodal perception

1313

$$\{\hat{y}_k\}, \{(\hat{s}_k, \hat{y}_k)\} \sim p_{\mathcal{M}_{n-1}^{\text{Perception}}}(\cdot \mid v_k, x)$$

1314

1315

- 13: Generate visual instruction responses: # Enhance multimodal reasoning

1316

$$\{\hat{a}_z\}, \{(\hat{r}_z, \hat{a}_z)\} \sim p_{\mathcal{M}_{n-1}^{\text{Reasoning}}}(\cdot \mid v_z, q)$$

1317

1318

- 14: Generate text-only responses: # Maintain language

1319

$$\{\hat{y}_t\} \sim p_{\mathcal{M}_{LLM}}(\cdot \mid x_t)$$

1320

1321

Step 3: Self-Consistency Selection

1322

- 16: Select the optimal candidates based on self-consistency, using the predefined threshold τ :

1323

1324

$$\mathcal{D}_{\text{Selected}}^{\text{Perception}} \leftarrow \arg \max_y \sum_j \text{sim}(y, y^{(j)}) \quad \text{s.t.} \quad \max_y \frac{1}{j} \sum_j \text{sim}(y, y^{(j)}) \geq \tau^{\text{Perception}}$$

1325

1326

$$\mathcal{D}_{\text{Selected}}^{\text{Reasoning}} \leftarrow \arg \max_a \sum_j \text{sim}(a, a^{(j)}) \quad \text{s.t.} \quad \max_a \frac{1}{j} \sum_j \text{sim}(a, a^{(j)}) \geq \tau^{\text{Reasoning}}$$

1327

1328

1329

$$\mathcal{D}_{\text{Selected}}^{\text{Language}} \leftarrow \arg \max_{y_t} \sum_j \text{sim}(y_t, y_t^{(j)}) \quad \text{s.t.} \quad \max_{y_t} \frac{1}{j} \sum_j \text{sim}(y_t, y_t^{(j)}) \geq \tau^{\text{Language}}$$

1330

1331

1332

- 17: Construct refined pre-training dataset:

1333

1334

$$\mathcal{D}^{\text{Pre-training}} = \mathcal{D}_{\text{Selected}}^{\text{Perception}} + \mathcal{D}_{\text{Selected}}^{\text{Reasoning}} + \mathcal{D}_{\text{Selected}}^{\text{Language}}$$

1335

1336

Step 4: Constructing the Next-Generation Foundation MLLM

1337

Stage 1: Modality Alignment

1338

1339

$$\mathcal{M}_n^1 \leftarrow \mathcal{L}_\phi^{\text{Stage 1}}(\mathcal{D}^{\text{Alignment}})$$

1340

1341

- 20: **Stage 1.5: Multimodal Pre-Training** # Pre-train on curated self-generated data

1342

1343

$$\mathcal{M}_n^{1.5} \leftarrow \mathcal{L}_\phi^{\text{Stage 1.5}}(\mathcal{D}^{\text{Pre-training}})$$

1344

1345

Stage 2: Visual Instruction-Tuning

1346

1347

$$\mathcal{M}_n^{\text{Next}} \leftarrow \mathcal{L}_\phi^{\text{Stage 2}}(\mathcal{D}^{\text{Instruction-Tuning}})$$

1348

22: **end for**

1349

23: **Output:** Next-generation foundation MLLM with self-improved cognition $\mathcal{M}_n^{\text{Next}}$

1350 **C MATHEMATICAL PROOF OF SICOG**
 1351

1352 **C.1 DEFINITIONS**
 1353

1354 To formalize the proof for this self-improving cycle, we establish the following definitions:
 1355

- 1356 • Let M_t be the base pre-trained model at the start of iteration t .
- 1357 • Let $D_{\text{pre},t}$ be the large-scale pre-training dataset used to train M_t from scratch.
- 1358 • Let D_A be a separate, high-quality annotated dataset used for capability enhancement via
 1359 fine-tuning.
- 1360 • Let M'_t be the enhanced model created by fine-tuning M_t on the dataset D_A . This model is
 1361 used for data generation but is discarded at the end of the iteration.
- 1362 • Let $D_{S,t}$ be the new dataset curated at iteration t by applying a quality filter to the outputs
 1363 of the **enhanced model** M'_t .
- 1364 • Let $D_{\text{pre},t+1}$ be the augmented pre-training dataset for the next iteration: $D_{\text{pre},t+1} =$
 1365 $D_{\text{pre},t} \cup D_{S,t}$.
- 1366 • Let M_{t+1} be the new base pre-trained model for the next iteration, produced by training a
 1367 model **from scratch** on the complete augmented dataset $D_{\text{pre},t+1}$.
- 1368 • Let $J(M)$ be the **capability** of a model M , defined as its expected true utility on a represen-
 1369 tative test distribution.
- 1370 • Let $U(D)$ be the average true utility of the examples within a dataset D .

1373 **C.2 THE ITERATIVE CYCLE**
 1374

1375 At each iteration t , the framework executes the following steps:
 1376

- 1377 1. **Capability Enhancement (Post-Training Optimization):** The current base model M_t is
 1378 fine-tuned on the high-quality dataset D_A to produce an enhanced model, M'_t .
- 1379 2. **Data Generation and Curation (Inference-Time Computation):** The enhanced model
 1380 M'_t is used to generate a large corpus of outputs. These are filtered to create a high-quality
 1381 curated dataset, $D_{S,t}$.
- 1382 3. **Corpus Augmentation:** The curated dataset $D_{S,t}$ is added to the previous pre-training
 1383 corpus $D_{\text{pre},t}$ to form a new, larger corpus $D_{\text{pre},t+1}$.
- 1384 4. **Re-training from Scratch:** A new base model, M_{t+1} , is initialized with random weights
 1385 and trained from scratch on the entire augmented dataset $D_{\text{pre},t+1}$.

1386 The objective remains to prove that this process ensures $J(M_{t+1}) \geq J(M_t)$.
 1387

1389 **C.3 CORE ASSUMPTIONS**
 1390

1392 The proof now relies on three fundamental assumptions.

1393 **Assumption 1** (Beneficial Fine-Tuning). Fine-tuning the base model M_t on the high-quality annotated
 1394 dataset D_A results in an enhanced model M'_t with capability that is greater than or equal to the
 1395 original model. This captures the benefit of the fine-tuning step.

$$1396 \quad J(M'_t) \geq J(M_t) \quad (25)$$

1398 **Assumption 2** (Effective Curation). The curation process is effective. It selects a subset of self-
 1399 generated data, $D_{S,t}$, whose average utility is strictly greater than the capability of the model that
 1400 generated it, which is now the **enhanced model** M'_t .

$$1401 \quad U(D_{S,t}) > J(M'_t) \quad (26)$$

1403 **Assumption 3** (Monotonic Pre-training on Augmented Data). This assumption remains the same but
 1404 is crucial. It posits that training a model from scratch on an augmented dataset results in a better (or

1404 equal) base model, provided the added data is of sufficiently high quality relative to the **original base**
 1405 **model** M_t .

$$1406 \text{ If } U(D_{S,t}) > J(M_t), \text{ then } J(M_{t+1}) \geq J(M_t) \quad (27)$$

1407 This assumption connects the quality of the new data to the improvement of the next-generation *base*
 1408 *model*.

1410 C.4 THE PROOF OF NON-DECREASING CAPABILITY

1412 We will now prove that $J(M_{t+1}) \geq J(M_t)$ by following the steps of the iterative self-improving
 1413 cycle.

- 1415 1. The process begins at iteration t with the base model M_t , which has capability $J(M_t)$.
- 1416 2. The model M_t is fine-tuned on D_A to create the enhanced model M'_t . By **Assumption 1**
 1417 **(Beneficial Fine-Tuning)**, we have:

$$1418 \quad J(M'_t) \geq J(M_t) \quad (28)$$

- 1420 3. The enhanced model M'_t is used to generate and curate the new dataset, $D_{S,t}$. By **Assump-**
 1421 **tion 2 (Effective Curation)**, the quality of this new data is superior to the capability of the
 1422 model that generated it:

$$1423 \quad U(D_{S,t}) > J(M'_t) \quad (29)$$

- 1424 4. We can now combine the inequalities from steps 2 and 3. From equation 29 and equation 28,
 1425 we can form a logical chain:

$$1427 \quad U(D_{S,t}) > J(M'_t) \geq J(M_t) \quad (30)$$

1428 This chain implies that the utility of the new data is strictly greater than the capability of the
 1429 *original base model*:

$$1430 \quad U(D_{S,t}) > J(M_t) \quad (31)$$

- 1432 5. A new base model, M_{t+1} , is then trained from scratch on the augmented pre-training corpus,
 1433 $D_{\text{pre},t+1} = D_{\text{pre},t} \cup D_{S,t}$.

- 1434 6. We are now in the exact scenario described by **Assumption 3 (Monotonic Pre-training on**
 1435 **Augmented Data)**. We have:

- 1436 • An original base model M_t .
- 1437 • A new base model M_{t+1} trained on $D_{\text{pre},t} \cup D_{S,t}$.
- 1438 • A guarantee from inequality equation 31 that the quality condition $U(D_{S,t}) > J(M_t)$
 1439 is met.
- 1440 7. Therefore, by directly applying **Assumption 3**, we can conclude that the capability of the
 1441 new base model is greater than or equal to the capability of the original base model:

$$1442 \quad J(M_{t+1}) \geq J(M_t) \quad (32)$$

1444 We have formally demonstrated that even with the intermediate fine-tuning step, the iterative self-
 1445 improving cycle ensures a monotonically non-decreasing sequence of **base model capabilities**. This
 1446 holds true as long as our three core assumptions are valid. The dataset D_A now plays a critical role
 1447 as an “enhancer” within the loop, helping to generate even higher-quality data ($D_{S,t}$) than the base
 1448 model could on its own, thereby driving the improvement of the entire system.

1458 **D DETAILED DISCUSSION ON RELATED WORK**
14591460 Table 5: Comparison of multimodal (vision-language) pre-training methods for enhancing multimodal
1461 capabilities. For VILA², ✓(✗) indicates a hybrid approach combining bootstrapped captions with
1462 fine-grained attributes from expert models. Detailed D (Detailed Description), DD-FGA (Detailed
1463 Description with Fine-Grained Attributes, Direct A (Direct Answer).
1464

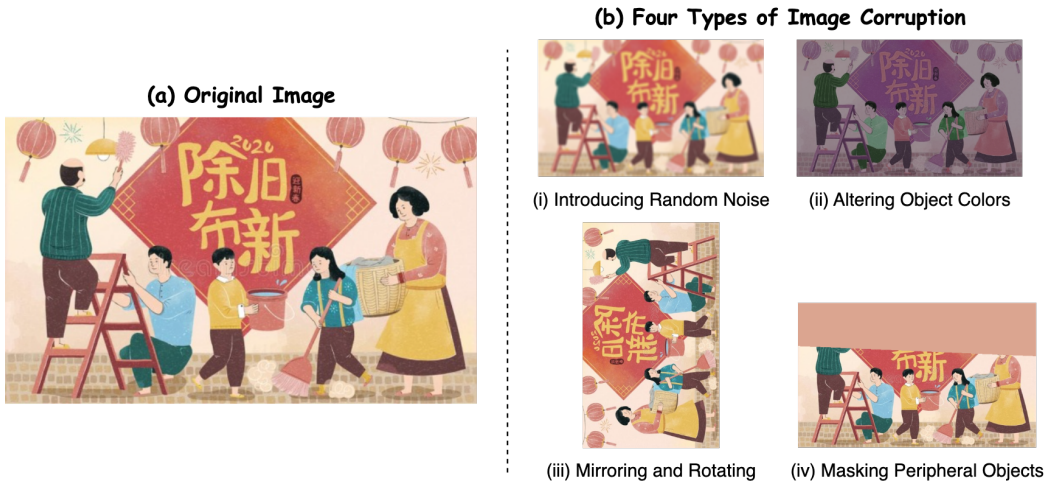
| 1465 1466 1467 1468 1469 1470 1471 1472 1473 1474 1475 1476 1477 1478 1479 1480 1481 1482 1483 1484 1485 1486 1487 1488 1489 1490 1491 1492 1493 1494 1495 1496 1497 1498 1499 1500 1501 1502 1503 1504 1505 1506 1507 1508 1509 1510 1511 | Method | w/o External Annotation | Caption Type | | VQA Type | |
|--|--------|----------------------------|--------------|-----|----------|-----|
| | | Detailed D | DD-FGA | CoD | Direct A | CoT |
| Detailed (Re-)Captioning (Perception) | | | | | | |
| ALLaVA (Chen et al., 2024a) | | ✗ | ✓ | | | |
| LLaVA-NeXT (Li et al., 2024a) | | ✗ | | | | |
| DCE (Sun et al., 2024) | | ✗ | | ✓ | | |
| MMGiC (Xu et al., 2024a) | | ✓(✗) | | ✓ | | |
| VILA ² (Fang et al., 2024) | | ✓(✗) | | ✓ | | |
| Detailed Re-Captioning & Visual Instruction Tuning (Perception & Reasoning) | | | | | | |
| SICOG (Ours) | | ✓ | ✓ | ✓ | ✓ | ✓ |

Improving multimodal perception abilities of MLLMs. Although MLLMs demonstrate strong multimodal perception capabilities (Liu et al., 2024a; Lu et al., 2024a), they often struggle with fine-grained tasks such as OCR (Fu et al., 2024b; Liu et al., 2024d; Yin et al., 2024; Lai et al., 2023; Li et al., 2024d; Peng et al., 2023). These challenges arise primarily from the reliance on popular large-scale caption datasets (*i.e.*, image-text pairs) (Sharma et al., 2018; Schuhmann et al., 2022; Changpinyo et al., 2021) for modality alignment, which often contain short, coarse-grained captions, restricting their ability to extract detailed visual information (Chen et al., 2024b;a; Lai et al., 2024). One common solution is additional pre-training with high-quality, detailed captions (Chen et al., 2024a; Li et al., 2024d; Lu et al., 2024a; Bai et al., 2023; Yu et al., 2024a) or captions enriched with fine-grained attributes (Xu et al., 2024a; Sun et al., 2024; Fang et al., 2024), improving their ability to capture visual details. In contrast, we propose *Chain-of-Description*, which explicitly models the perception process. This approach trains models to systematically acquire and interpret visual information through step-by-step analysis and decomposition of complex scenes, enabling deeper understanding of fine-grained details.

Improving multimodal reasoning abilities of MLLMs. Complex multimodal reasoning tasks that require integrating visual information into reasoning processes, such as mathematical computation, present significant challenges for MLLMs (Yue et al., 2024b; Chen et al., 2024d; Hao et al., 2025; Xu et al., 2025). Recent studies (Chen et al., 2024d; Cheng et al., 2024; Zhang et al., 2024c) enhance reasoning capabilities by incorporating chain-of-thought (CoT) reasoning (Wei et al., 2022; Zhang et al., 2023), prompting or fine-tuning models to generate intermediate reasoning steps before producing final answers. Structured and systematic extensions of CoT (Xiang et al., 2024; Xu et al., 2025; Cheng et al., 2024; Dong et al., 2024) further improve performance through step-by-step logical processes. While these approaches prove effective during post-training, we investigate incorporating CoT reasoning during pre-training, recognizing this stage as foundational to MLLMs' overall capabilities.

1512 **E CAN PREFERENCE LEARNING SUPPORT SICOG’S SYSTEMATIC**
 1513 **PERCEPTION AND REASONING DEVELOPMENT?**

1516 Motivated by the great success of preference learning in adapting MLLMs to follow instructions
 1517 during the post-training stage (Rafailov et al., 2023; Zhang et al., 2024a), we explore its application
 1518 to enhance MLLM’s multimodal perception and reasoning capabilities during Step 1 of SICOG
 1519 (Section 3). Specifically, we construct preference caption pairs by using high-quality captions from the
 1520 annotated caption dataset (Section 3) as preferred captions and pairing them with corresponding low-
 1521 quality (dispreferred) captions. The low-quality captions are generated by corrupting the associated
 1522 images through the following methods (Figure 5): (i) introducing random noise to hinder key
 1523 information capture, (ii) altering object colors to disrupt fine-grained detail perception, (iii) mirroring
 1524 and rotating images to distort relation-level attributes, and (iv) masking peripheral objects to obscure
 1525 peripheral content. We fine-tune the MLLM on these caption preference pairs using the Direct
 1526 Preference Optimization (DPO) algorithm (Rafailov et al., 2023) to initialize systematic perception
 1527 capabilities. Similarly, we extend preference learning to develop systematic reasoning capabilities.



1544 Figure 5: Illustration of (a) the original image and (b) the four types of image corruption.
 1545

1546 **Preference learning supports SICOG’s systematic perception and reasoning development.** As
 1547 shown in Table 6, preference learning with DPO significantly enhances MLLMs’ systematic percep-
 1548 tion and reasoning, enabling their self-improvement via SICOG, *e.g.*, achieving a 2.5% accuracy gain
 1549 on MMstar.

1550 Table 6: Evaluation results of different training methods for developing perception and reasoning in
 1551 LLaVA-Qwen2-7B during Step 1 of SICOG (post-training optimization, Section 3).

| Method | Capability Development | Comprehensive | | | Hallu. Chart & Table | | | Knowledge | | |
|--|------------------------|---------------|--------------|--------------|----------------------|--------------|--------------|--------------|--------------|--------------|
| | | MMBen. | MMStar | MMVet | POPE | DocV. | Chart. | Math. | Science. | AI2D |
| Base Model | | | | | | | | | | |
| LLaVA-Qwen2-7B | - | 74.44 | 46.67 | 38.85 | 84.55 | 50.62 | 52.72 | 38.00 | 74.91 | 73.77 |
| Self-Improving Cognition | | | | | | | | | | |
| SICOG-LLaVA-Qwen2-7B (Per., Rea., Lan.) | SFT (Per., Rea.) | 75.45 | 48.60 | 37.84 | 84.35 | 52.52 | 54.48 | 38.80 | 77.44 | 76.20 |
| | DPO (Per., SFT (Rea.)) | 76.18 | 48.40 | 38.72 | 83.53 | 52.20 | 54.80 | 39.20 | 77.49 | 75.78 |
| | DPO (Per., Rea.) | 74.83 | 49.00 | 38.90 | 84.85 | 52.54 | 55.64 | 41.00 | 76.20 | 76.33 |

1562 **Preference learning is more effective than supervised fine-tuning for systematic perception and**
 1563 **reasoning development.** Preference learning with DPO consistently surpasses standard supervised
 1564 fine-tuning across all benchmarks for initializing systematic perception and reasoning in SICOG.
 1565 For example, on MathVista, preference learning improves accuracy by approximately 2% on the
 low-resolution model LLaVA-Qwen2-7B, which is particularly challenging to enhance due to inherent

1566 visual perception limitations. These results underscore the importance of learning not only from
 1567 correct examples but also from avoiding mistakes, thereby fostering more robust skill development.
 1568

1569 **F HOW DOES SICOG ENHANCE THE REASONING CAPABILITIES OF**
 1570 **FOUNDATION MLLMs?**

1573 Table 7: Evaluation results of SICOG variants on LLaVA-Qwen2-7B-UHD in two inference settings:
 1574 direct answer and CoT for reasoning abilities.

| Method | Infer. | Train Data Stage 2 | Comprehensive | | | Hallu. | Chart/Table | Knowledge | | | |
|---|--------|---------------------------------------|---------------|--------------|--------------|--------------|--------------|--------------|--------------|--------------|--------------|
| | | | MMBench | MMStar | MMVet | | | POPE | DocV. | Chart. | |
| Base Model | | | | | | | | | | | |
| LLaVA-Qwen2-7B-UHD | Direct | - | 77.63 | 48.93 | 38.26 | 87.31 | 70.18 | 69.96 | 38.90 | 77.29 | 74.94 |
| Self-Improving Cognition | | | | | | | | | | | |
| SICOG-LLaVA-Qwen2-7B-UHD (Perception, Reasoning, Language) | Direct | - | 77.80 | 52.47 | 40.14 | 87.84 | 73.05 | 72.24 | 41.40 | 79.42 | 78.40 |
| | Direct | + Self-generated 45k VQA w/ DA&CoT | 76.12 | 51.00 | 39.82 | 88.02 | 74.15 | 73.12 | 42.90 | 80.61 | 78.21 |
| | CoT | + Self-generated 45k VQA w/ DA&CoT | 65.19 | 44.60 | 40.92 | 87.36 | 72.48 | 76.20 | 36.90 | 72.93 | 73.19 |

1585 **Quantitative Analysis.** We validate the efficacy of SICOG (perception, reasoning, language) in
 1586 enhancing the reasoning capabilities of MLLMs under two inference settings: direct answer and CoT.
 1587 The absence of CoT reasoning annotations in the instruction-tuning data (Zhang et al., 2024b; Liu
 1588 et al., 2024a) used in stage 2 limits the model’s ability to generate CoT reasoning. To address this
 1589 limitation, we incorporate 45k self-generated visual instruction-tuning examples—originally used
 1590 during the pre-training stage (stage 1.5)—into the instruction-tuning stage (stage 2) (see details in
 1591 step 4 of section 3).

1592 **Incorporating self-generated visual instruction-tuning data for instruction-tuning further im-
 1593 proves multimodal reasoning.** As shown in Table 7, incorporating self-generated visual instruction-
 1594 tuning data in stage 2 enhances SICOG’s performance on most reasoning-intensive tasks across both
 1595 inference settings. For instance, it provides an additional accuracy gain of approximately 1-4%
 1596 on ChartQA. On benchmarks such as POPE and ScienceQA, direct answer inference outperforms
 1597 CoT inference, likely due to the overwhelming prevalence of direct answer annotations compared
 1598 to CoT annotations in the instruction-tuning data. In addition, we observe a performance drop on
 1599 perception-heavy benchmarks like MMBench and MMStar. We suspect this decline stems from a
 1600 data distribution shift introduced by the additional reasoning-focused data.

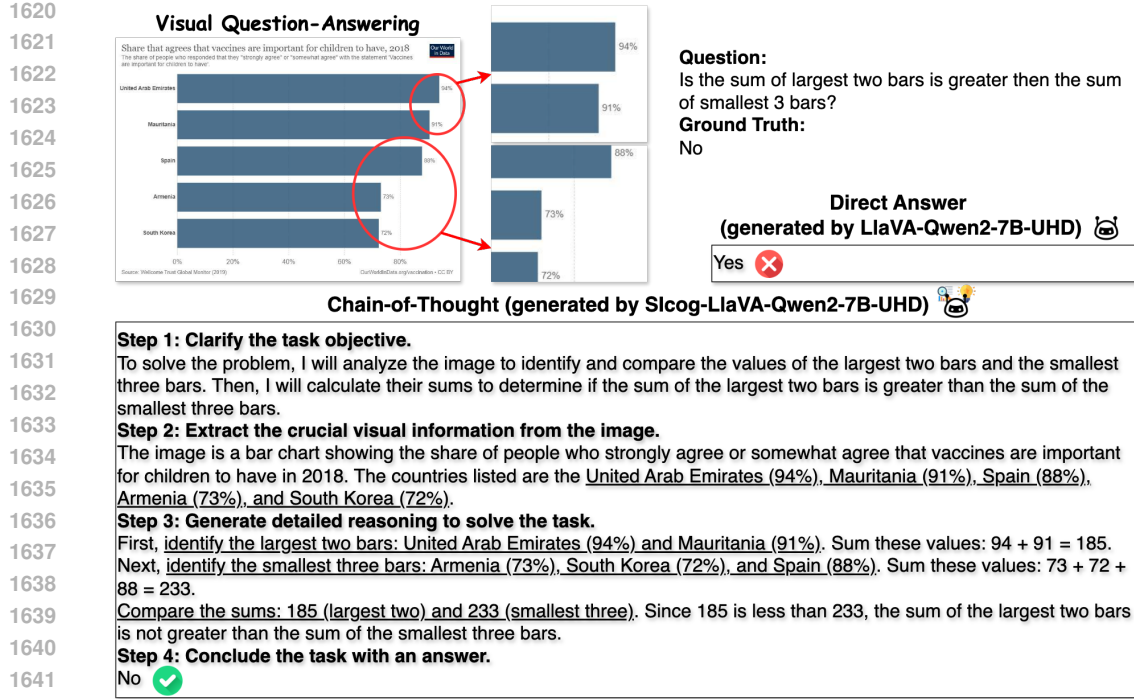


Figure 6: Qualitative comparison of responses generated by LLaVA-Qwen2-7B-UHD and SICOG-LLaVA-Qwen2-7B-UHD for the visual instruction-following task.

Qualitative Analysis. We compare the responses generated by the base LLaVA-Qwen2-7B-UHD and SICOG-LLaVA-Qwen2-7B-UHD (enhanced with self-generated VQA data in Stage 2) on an image-question pair from ChartVQA.

Figure 6 illustrates that, unlike LLaVA-Qwen2-7B-UHD, which produces an incorrect answer, SICOG-LLaVA-Qwen2-7B-UHD effectively integrates multimodal information into a systematic reasoning process, yielding an accurate and coherent response. Specifically, SICOG-LLaVA-Qwen2-7B-UHD first clarifies the task requirements and extracts key visual information, such as "United Arab Emirates (94%)" and "Mauritania (91%)". It then systematically leverages this information, identifying the two largest bars—United Arab Emirates (94%) and Mauritania (91%)—and the three smallest bars—Armenia (73%), South Korea (72%), and Spain (88%). By performing precise reasoning and calculations, SICOG-LLaVA-Qwen2-7B-UHD ultimately derives the correct answer. These findings confirm the efficacy of SICOG in enhancing the systematic reasoning capabilities of MLLMs, aligning with the results observed in the quantitative analysis.

1674 G HOW DOES SCALING SELF-GENERATED PRE-TRAINING DATA AFFECT 1675 THE PERFORMANCE OF SICOG?

1678 The primary objective of multimodal pre-training
 1679 is to refine and enhance knowledge acquisition
 1680 from image captioning datasets (Li et al., 2024a).
 1681 In this context, we analyze the effect of scaling
 1682 self-generated pre-training data on SICOG-LLaVA-
 1683 Qwen2-7B-UHD (perception, reasoning, language)
 1684 by prioritizing an increase in the number of self-
 1685 generated caption data. Specifically, we assess the
 1686 performance of SICOG across four dimensions on
 1687 ten benchmarks: comprehensive understanding (MM-
 1688 Bench, MMStar, MMVet), hallucination (POPE),
 1689 OCR and chart/table understanding (OCRBench,
 1690 DocVQA, ChartQA), and knowledge-intensive tasks
 1691 (MathVista, ScienceQA, AI2D) (Figure 7).

1692 **Scaling up self-generated captions improves the**
 1693 **performance of SICOG.** Increasing the quantity
 1694 of self-generated caption data results in consistent
 1695 performance improvements across three dimensions:
 1696 comprehensive understanding (up to approximately
 1697 2%), OCR and chart/table understanding (up to
 1698 around 2.5%), and knowledge-intensive tasks (up to
 1699 around 3%), while maintaining stable performance on
 1700 hallucination tasks. These improvements underscore
 1701 the importance of scaling caption data in enhancing
 1702 SICOG’s ability to improve MLLMs’ multimodal cog-
 1703 nition. However, a slight performance decline occurs when the amount of caption data is increased
 1704 without proportionally adjusting the quantities of visual and text-only instruction tuning data. We
 1705 hypothesize that this decline arises from the overwhelming dominance of caption data, which creates
 1706 an imbalanced data ratio and hinders effective model optimization.

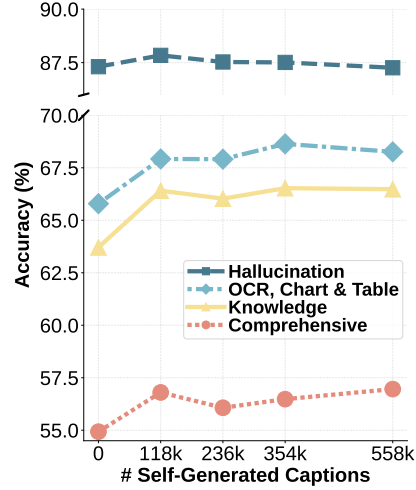
1707 H DOES SICOG REMAIN EFFECTIVE WHEN VARYING RECAPTIONED 1708 IMAGES?

1709
 1710 Table 8: Evaluation results of varying unlabeled image datasets for recaptioning on SICOG-LLaVA-
 1711 Qwen2-7B-UHD across eleven benchmarks.

| Method | Comprehensive | | Hallu. | | Chart & Table | | Knowledge | | Vision | | |
|---|---------------|--------------|--------------|--------------|---------------|--------------|--------------|--------------|--------------|--------------|--------------|
| | MMBen. | MMStar | MMVet | POPE | OCR | DocV. | Chart. | Math. | Science. | AI2D | Realworld. |
| <i>Base Model</i> | | | | | | | | | | | |
| LLaVA-Qwen2-7B-UHD | 77.63 | 48.93 | 38.26 | 87.31 | 55.20 | 70.18 | 69.96 | 38.90 | 77.29 | 74.94 | 63.53 |
| <i>Self-Improving Cognition</i> | | | | | | | | | | | |
| SICOG-LLaVA-Qwen2-7B-UHD (P., R., L.) (Recap. w/ BLIP 118k (Li et al., 2022)) | 77.80 | 52.47 | 40.14 | 87.84 | 57.70 | 73.05 | 72.24 | 41.40 | 79.42 | 78.40 | 63.92 |
| SICOG-LLaVA-Qwen2-7B-UHD (P., R., L.) (Recap. w/ V-FLAN 148k (Xu et al., 2024b)) | 77.07 | 51.93 | 38.67 | 87.50 | 56.40 | 73.45 | 73.60 | 40.20 | 79.38 | 77.85 | 67.19 |

1721 We validate the effectiveness of SICOG across varying corpora by employing different unlabeled
 1722 image datasets for recaptioning. Specifically, we randomly sample 148k images from the Vision-Flan
 1723 (V-Flan) dataset (Xu et al., 2024b), which provides a diverse range of images and ensures zero overlap
 1724 with the curated data described in Section 3.

1725 **SICOG is robust to variations in recaptioned images.** As shown in Table 8, SICOG-LLaVA-
 1726 Qwen2-7B-UHD (Perception, Reasoning, Language) consistently outperforms the base model,
 1727 LLaVA-Qwen2-7B-UHD, achieving an approximate 4% accuracy gain on RealworldQA. This result

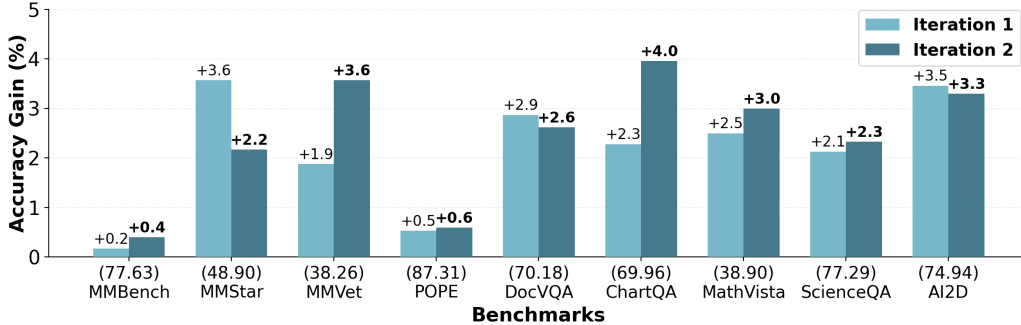


1728 Figure 7: Impact of scaling self-generated
 1729 captions on SICOG-LLaVA-Qwen2-7B-UHD
 1730 during multimodal pre-training, evaluated
 1731 across four dimensions on ten benchmarks.

underscores the role of image diversity in enhancing real-world understanding and demonstrates the robust generalizability of SICOG across different corpora.

1728
1729
1730
1731
1732
1733
1734
1735
1736
1737
1738
1739
1740
1741
1742
1743
1744
1745
1746
1747
1748
1749
1750
1751
1752
1753
1754
1755
1756
1757
1758
1759
1760
1761
1762
1763
1764
1765
1766
1767
1768
1769
1770
1771
1772
1773
1774
1775
1776
1777
1778
1779
1780
1781

1782 **I CAN SICOG CONTRIBUTE TO THE CONSTRUCTION OF NEXT-GENERATION**
 1783 **FOUNDATION MLLMs THROUGH CONTINUOUS COGNITIVE**
 1784 **SELF-IMPROVEMENT?**



1798 Figure 8: Evaluation results for next-generation foundation MLLM construction through continuous
 1799 self-improvement using SICOG. Accuracy gains are reported as absolute improvements over the base
 1800 model LLaVA-Qwen2-7B-UHD, with the base model’s performance shown in parentheses.
 1801

1802 The multimodal pre-training stage is specifically designed to expand the model’s knowledge base Liu
 1803 et al. (2024b). In this paper, we explore how self-learning can help expand the model’s knowledge base
 1804 during multimodal pre-training. We investigate the potential of SICOG in advancing next-generation
 1805 foundational MLLM construction through continuous cognitive self-improvement. Specifically, we
 1806 consider SICOG-LLaVA-Qwen2-7B-UHD (perception, cognition, language) from Table 1 as the
 1807 foundational MLLM obtained in the first iteration. In the second iteration, 148K images from the
 1808 V-Flan dataset are newly recaptioned, resulting in a self-curated dataset comprising caption data
 1809 (118K from BLIP and 148K from V-Flan), VQA data (45K), and textual QA data (50K).
 1810

1811 **SICOG drives next-generation foundational MLLM construction via continuous cognitive self-
 1812 improvement.** Figure 8 presents absolute accuracy gains over the initial base MLLM, LLaVA-Qwen2-
 1813 7B-UHD. The results show that SICOG-LLaVA-Qwen2-7B-UHD improves MLLM cognition across
 1814 most benchmarks in the second iteration, achieving an additional 1.5% accuracy gain on MMVet.
 1815 However, performance regressions on certain benchmarks may stem from an overrepresentation of
 1816 caption data.
 1817

1836 **J HOW DO *Chain-of-Description* AND CHAIN-OF-THOUGHT IMPROVE**
 1837 **COGNITION?**

1839 We examine two key factors underlying SICOG’s efficacy: (i) the role of *Chain-of-Description*
 1840 in facilitating multimodal perception, and (ii) the contribution of structured chain-of-thought to
 1841 multimodal reasoning.

1843 **J.1 HOW DOES *Chain-of-Description* FACILITATE MULTIMODAL PERCEPTION?**

1845 **Quantitative Analysis.** We analyze captions for 100 images randomly sampled from BLIP-558k (Li
 1846 et al., 2022), which is used as unlabeled image captioning data in Section 4. These captions are gen-
 1847 erated by perception-enhanced models fine-tuned on annotated caption data in three formats: detailed
 1848 description (Detailed D), *Chain-of-Description* (CoD), and their combination (as implemented in
 1849 SICOG, described in Section 3). Using GPT-4 with the prompt shown in Table 21, we evaluate six
 1850 key dimensions: salient content, fine-grained details, relational attributes, peripheral content, faith-
 1851 fulness, and world knowledge. For a holistic analysis, we also include LLaVA-NeXT-34B, a leading
 1852 open-source MLLM known for its strong captioning capabilities (Li et al., 2024a). Table 9 shows that
 1853 the base model, regardless of resolution, consistently underperforms in salient content, fine-grained
 1854 details, relational attributes, and peripheral content. These results highlight the importance of the
 1855 four-step perception analysis design used in *Chain-of-Description*.

1856 Table 9: Evaluation of re-captioning quality comparing the perception-enhanced models fine-tuned
 1857 on curated caption data in three formats: detailed description (Detailed D), *Chain-of-Description*
 1858 (CoD), and their combination (Section 3). Metrics (rated 1-5): salient content, fine-grained details,
 1859 relational attributes, peripheral content, faithfulness, and world knowledge. “Caption”: standard
 1860 format; “Multi.”: CoD step-by-step format (see Table 11 for details).

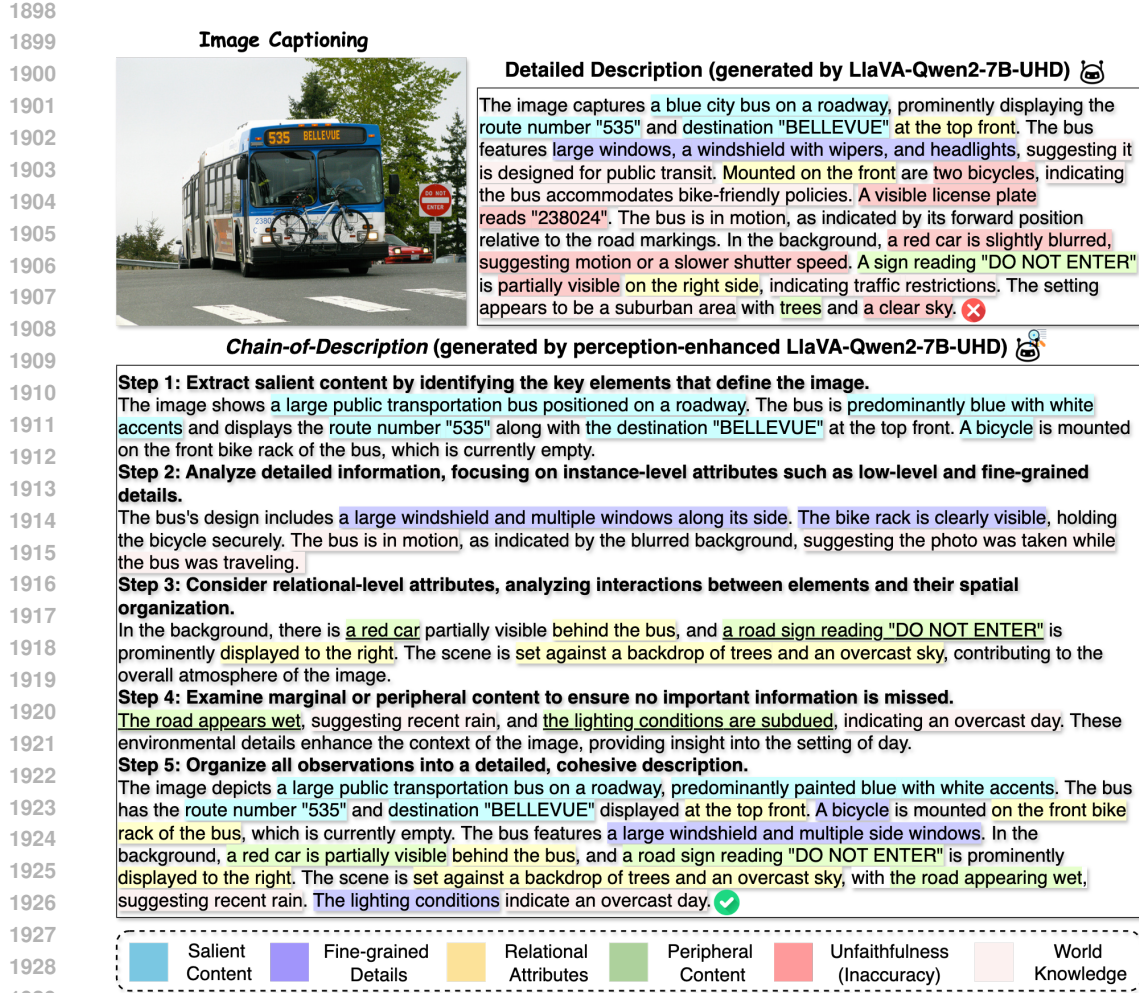
| Method | # Avg. Tokens | Systematic Perception | | | | General Performance | |
|---|------------------|-----------------------|-------------|-------------|-------------|---------------------|-------------|
| | | Sali. | Fine-Grain. | Rela. | Peri. | Faith. | Know. |
| Low-Resolution | | | | | | | |
| LLaVA-Qwen2-7B | 129.36 | 4.51 | 4.21 | 3.82 | 3.67 | 4.07 | 3.63 |
| + Finetune w/ Detailed D | 129.68 | 4.59 | 4.49 | 3.88 | 3.88 | 4.13 | 3.87 |
| + Finetune w/ CoD (Caption) | 130.55 | 4.73 | 4.52 | 4.06 | 3.92 | 4.36 | 3.90 |
| + Finetune w/ CoD (Multi.) | 458.09 | 4.71 | 4.69 | 4.62 | 4.22 | 4.32 | 4.01 |
| + Finetune w/ Detailed D & CoD (Detailed D) | 130.13 | 4.75 | 4.54 | 4.13 | 3.97 | 4.49 | 3.95 |
| + Finetune w/ Detailed D & CoD (CoD Multi.) | 436.53 | 4.89 | 4.81 | 4.76 | 4.26 | 4.67 | 4.05 |
| High-Resolution | | | | | | | |
| LLaVA-Qwen2-7B-UHD | 135.08 | 4.77 | 4.30 | 3.99 | 3.81 | 4.41 | 3.84 |
| + Finetune w/ Detailed D | 140.73 | 4.71 | 4.52 | 3.92 | 3.91 | 4.20 | 3.77 |
| + Finetune w/ CoD (Caption) | 126.93 | 4.78 | 4.58 | 4.11 | 3.90 | 4.57 | 3.93 |
| + Finetune w/ CoD (Multi.) | 453.13 | 4.82 | 4.80 | 4.74 | 4.29 | 4.57 | 4.01 |
| + Finetune w/ Detailed D & CoD (Detailed D) | 136.50 | 4.76 | 4.67 | 4.01 | 3.82 | 4.51 | 3.88 |
| + Finetune w/ Detailed D & CoD (CoD Multi.) | 453.26 | 4.91 | 4.87 | 4.78 | 4.32 | 4.71 | 4.05 |
| LLaVA-NeXT-34B (Liu et al., 2024b) | 206.50 | 4.77 | 4.51 | 4.04 | 3.95 | 4.59 | 4.12 |

1878 **Chain-of-Description shows strong efficacy in facilitating systematic perception across six key**
 1879 **dimensions.** Perception-enhanced models fine-tuned with *Chain-of-Description* outperform those
 1880 trained on detailed descriptions in both single-step (caption-only) and multi-step formats. Notably,
 1881 their combination achieves the highest evaluation scores, surpassing LLaVA-NeXT-34B in five of the
 1882 six dimensions.

1883 Furthermore, *Chain-of-Description* generates the longest average caption lengths (approximately
 1884 430–450 tokens), indicating a robust perceptual capacity. Additional analysis is provided in Ap-
 1885 pendix L.

1886 **Qualitative Analysis.** We compare two caption examples generated by LLaVA-Qwen2-7B-UHD
 1887 and perception-enhanced LLaVA-Qwen2-7B-UHD (adopted in SICOG) on an image from V-FLAN
 1888 148k, as referenced in Table 8.

1890 In Figure 9, the results reveal that *Chain-of-Description* enables MLLMs to capture richer and
 1891 more detailed visual information across all six dimensions, whereas captions generated by the base
 1892 LLaVA-Qwen2-7B-UHD often include inaccuracies, *e.g.*, hallucinations (Bai et al., 2024). For
 1893 instance, *Chain-of-Description* allows MLLMs to identify nuanced details such as “the road appears
 1894 wet” and “the lighting conditions are subdued” in step 4, suggesting “recent rain” and an “overcast
 1895 day.” In contrast, the base LLaVA-Qwen2-7B-UHD fails to capture these details, resulting in an
 1896 inaccurate description of “a clear sky.” This observation aligns with quantitative findings, confirming
 1897 *Chain-of-Description*’s effectiveness in enhancing systematic perception.



1938 Figure 9: Qualitative comparison of captions generated by LLaVA-Qwen2-7B-UHD and perception-
 1939 enhanced LLaVA-Qwen2-7B-UHD across six key dimensions in the image captioning task.

1940 **Chain-of-Description avoids redundancy through systematic step-wise analysis.** While *Chain-of-Description*
 1941 generates comprehensive and detailed descriptions, it maintains efficiency by *eliminating information overlap* in its step-by-step analysis. For instance, peripheral elements such as “a red car” and “a road sign reading ‘do not enter’” are described with precise spatial relations in step 3. Subsequently, step 4 focuses exclusively on new observations, such as “the road appears wet,” ensuring non-redundant content progression and avoiding verbosity.

1942 J.2 HOW DOES STRUCTURED CHAIN-OF-THOUGHT ENHANCE MULTIMODAL REASONING?

1943 **Quantitative Analysis.** We evaluate the accuracy of answers for 1k image-question pairs randomly
 1944 sampled from the 63k LLaVA-CoT split, which is used as unlabeled pre-training VQA data in
 1945 Section 4. These answers are generated by reasoning-enhanced models fine-tuned on curated

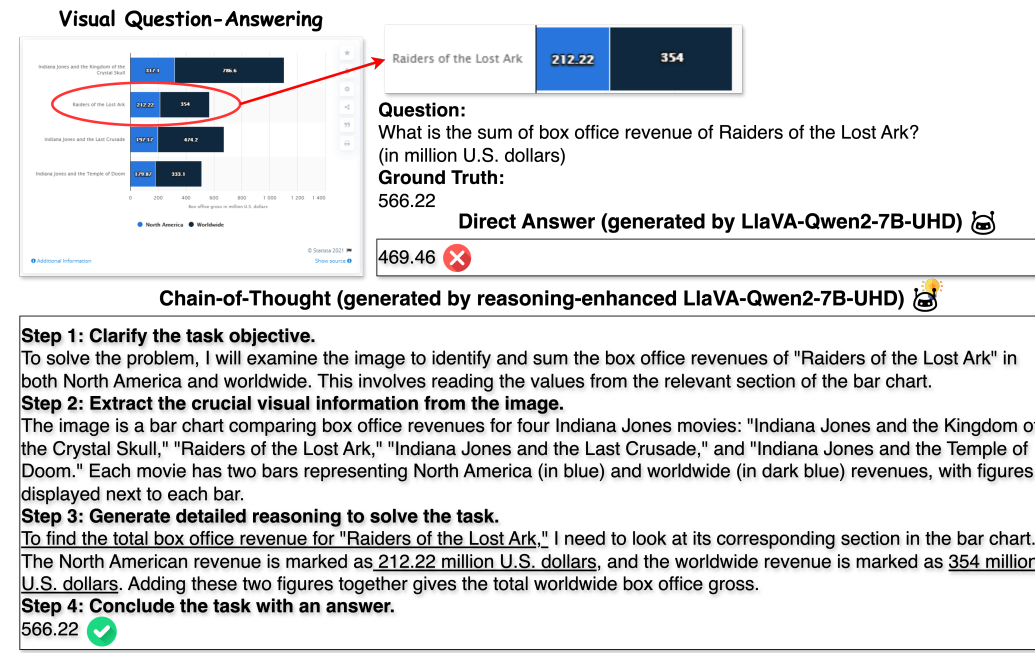
1944 reasoning data in three formats: direct answer, structured CoT, and their combination (as implemented
 1945 in SICOG). As shown in Table 10, models fine-tuned with structured CoT improve the base models'
 1946 performance by 9% in EM. The combination of CoT and direct answer achieves the best results,
 1947 outperforming other methods by 2% to 5% EM, demonstrating the effectiveness of structured CoT in
 1948 enhancing multimodal reasoning in MLLMs. However, models fine-tuned solely with CoT perform
 1949 comparably or slightly worse than those fine-tuned with direct answers, likely due to insufficient CoT
 1950 reasoning data in the base models' training set.

1951
 1952 Table 10: Evaluation of self-generated reasoning quality, comparing reasoning-improved models
 1953 fine-tuned on curated reasoning data in three formats: direct answer (Direct), chain-of-thought (CoT),
 1954 and their combination (Section 3). Exact Match (EM) scores are used to assess the correctness of
 1955 final answers.

| Low-Resolution | | High-Resolution | |
|--|---------------|--|---------------|
| Method | Correct. (EM) | Method | Correct. (EM) |
| LLaVA-Qwen2-7B | 26 | LLaVA-Qwen2-7B-UHD | 33 |
| + Finetune w/ Direct Answer | 35 | + Finetune w/ Direct Answer | 43 |
| + Finetune w/ Chain-of-Thought (CoT) | 35 | + Finetune w/ Chain-of-Thought (CoT) | 42 |
| + Finetune w/ Direct Ans. & CoT (Direct) | 37 | + Finetune w/ Direct Ans. & CoT (Direct) | 47 |
| + Finetune w/ Direct Ans. & CoT (CoT) | 37 | + Finetune w/ Direct Ans. & CoT (CoT) | 47 |

1963
 1964 **Qualitative Analysis.** We compare the responses generated by the base LLaVA-Qwen2-7B-UHD
 1965 and the reasoning-enhanced LLaVA-Qwen2-7B-UHD (used in SICOG) on an image-question pair
 1966 from the 63k LLaVA-CoT split.

1967 In Figure 10, our analysis demonstrates that the structured CoT enables the MLLM to generate
 1968 systematic, logical, and in-depth reasoning step-by-step, resulting in accurate answers. Specifically,
 1969 CoT first helps clarify the task requirements and captures critical visual information. Then, CoT
 1970 enables the MLLM to utilize key visual details, such as “212.22 million U.S. dollars” and “354
 1971 million U.S. dollars,” to perform accurate reasoning and calculations.



1997 Figure 10: Qualitative comparison of responses generated by LLaVA-Qwen2-7B-UHD and reasoning-enhanced LLaVA-Qwen2-7B-UHD in the visual question-answering task.

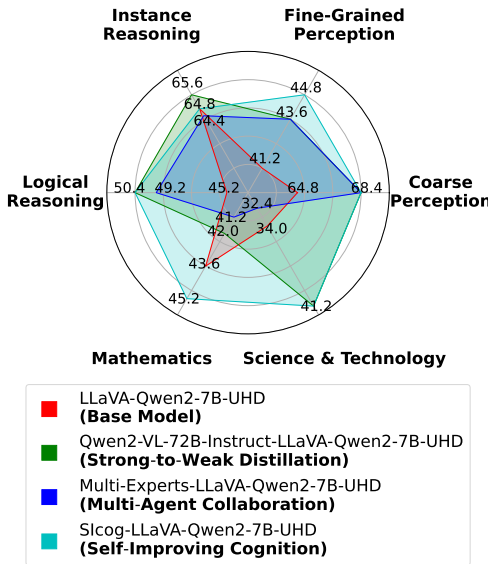
1998 K FINE-GRAINED EVALUATION ACROSS SIX CORE CAPABILITIES
1999
2000
2001
2002
2003
2004
2005
2006
2007
2008
2009
2010
2011
2012
2013
2014
2015
2016
2017
2018
2019
2020
2021
2022
2023
2024
2025
2026
2027
2028

Figure 11: Fine-grained evaluation of six core capabilities on LLaVA-Qwen2-7B-UHD using the MMStar benchmark (direct answer).

The fine-grained evaluation of six core capabilities in Figure 11 highlights the effectiveness of SICOG in advancing multimodal cognitive abilities in MLLMs.

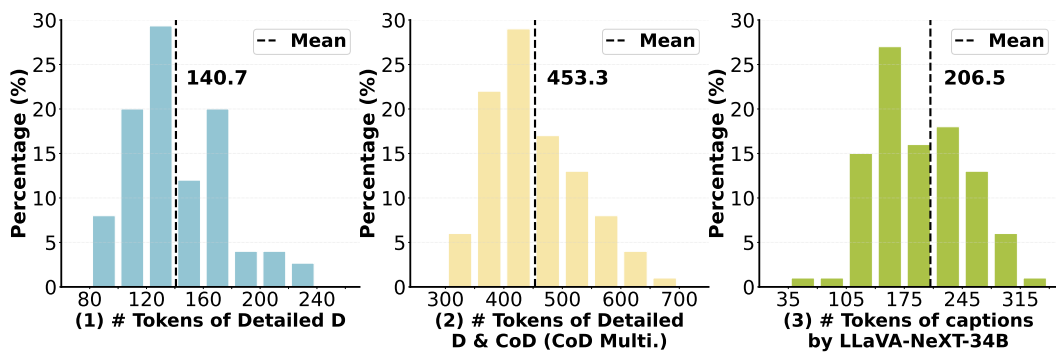
L DISTRIBUTION OF GENERATED CAPTION TOKEN LENGTHS
2029
2030
2031
2032
2033
2034
2035
2036
2037
2038
2039

Figure 12: Distribution of caption token lengths: perception-enhanced LLaVA-Qwen2-7B-UHD (fine-tuned on curated captions using the standard detailed description format and the mixture of detailed description and *Chain-of-Description* formats) vs. LLaVA-NeXT-34B.

Figure 12 compares token length distributions, showing that *Chain-of-Description* consistently produces longer captions across all images, suggesting a robust perceptual ability.

2052 **M IMPLEMENTATION DETAILS**

2053
2054 Table 11: Three different caption formats used for Chain-of-Description conversion during the
2055 multimodal pre-training stage (1/2).
2056

2057 **Three Caption Formats for Chain-of-Description Conversion in Multimodal Pre-Training**

2058 **Format 1: Standard caption-only.**

2059 **Human:** <image>\nPlease provide a thorough description of this image.

2060 **Model:** The image showcases a modern spiral staircase with a unique design. The staircase
2061 features a curved, wooden handrail that is dark brown in color, contrasting with the lighter wooden
2062 steps. The railings are made of the same dark wood and have a horizontal slat design, giving
2063 a sense of movement along the staircase's curve. The staircase itself appears to be constructed
2064 from polished wood, giving it a sleek and contemporary look. Below the staircase, the flooring
2065 is light beige, complementing the warm tones of the wooden staircase. The room surrounding
2066 the staircase is spacious, with large windows that allow natural light to enter, enhancing the
2067 brightness of the space. There are no people or objects in the immediate vicinity of the staircase,
2068 emphasizing the architectural features. The overall color scheme is warm, with the wood tones
2069 being the dominant feature.

2070 **Format 2: Step-by-step elicitation.**

2071 **Human:** <image>\nPlease provide a thorough description of this image. Explain your description
2072 step by step.

2073 **Model:** Step 1: Extract salient content by identifying the key elements that define the image.

2074 The image depicts a modern spiral staircase with a striking design. The staircase features a curved,
2075 wooden handrail that is dark brown in color, contrasting with the lighter wooden steps. The
2076 railings are made of the same dark wood and have a horizontal slat design, providing a sense of
2077 movement along the staircase's curve.

2078 Step 2: Analyze detailed information, focusing on instance-level attributes such as low-level and
2079 fine-grained details.

2080 The staircase is constructed from polished wood, which gives it a sleek and contemporary
2081 appearance. The flooring below the staircase is light beige, complementing the warm tones of the
2082 wooden staircase. The room surrounding the staircase is spacious, with large windows that allow
2083 natural light to enter, enhancing the brightness of the space.

2084 Step 3: Consider relational-level attributes, analyzing interactions between elements and their
2085 spatial organization.

2086 The staircase's design is both functional and aesthetic, with its spiral form creating a dynamic
2087 visual element within the room. The natural light from the windows highlights the warm tones of
2088 the wood and adds depth to the space. The absence of people or objects in the room emphasizes
2089 the architectural features of the staircase.

2090 Step 4: Examine marginal or peripheral content to ensure no important information is missed.

2091 The room's architecture is modern, with clean lines and minimalistic design elements. The
2092 combination of the staircase's curved form and the natural light creates an inviting and open
2093 atmosphere in the space.

2094 Step 5: Organize all observations into a detailed, cohesive description.

2095 The image showcases a modern spiral staircase with a unique design. The staircase features a
2096 curved, wooden handrail that is dark brown in color, contrasting with the lighter wooden steps.
2097 The railings are made of the same dark wood and have a horizontal slat design, giving a sense of
2098 movement along the staircase's curve. The staircase itself appears to be constructed from polished
2099 wood, giving it a sleek and contemporary look...

2096 **M.1 COMPARED METHODS.**

2099 We compare SICOG against the following representative MLLM pre-training approaches (as discussed
2100 in Section 2). Differences are considered significant at $p < 0.01$:

2101
2102
2103
2104
2105

- **Strong-to-Weak Distillation (Perception)** (Li et al., 2024a): Pre-training with re-caption data
containing detailed descriptions (DD) generated by stronger models.
- **Multi-Agent Collaboration (Perception)** (Fang et al., 2024): Pre-training with re-caption data
containing detailed descriptions and fine-grained attributes (DD-FGA) generated by base and
expert models.

2106 Table 12: Three different caption formats used for Chain-of-Description conversion during the
 2107 multimodal pre-training stage (2/2).

2109 **Three Caption Formats for Chain-of-Description Conversion in Multimodal Pre-Training**

2110 **Format 3: Multi-turn conversation.**

2111 **Human:** <image>\nWhat are the crucial details that define the image?

2112 **Model:** The image depicts a modern spiral staircase with a striking design. The staircase features
 2113 a curved, wooden handrail that is dark brown in color, contrasting with the lighter wooden steps.
 2114 The railings are made of the same dark wood and have a horizontal slat design, providing a sense
 2115 of movement along the staircase’s curve.

2116 **Human:** Can you analyze the image for instance-level attributes and low-level details?

2117 **Model:** The staircase is constructed from polished wood, which gives it a sleek and contemporary
 2118 appearance. The flooring below the staircase is light beige, complementing the warm tones of the
 2119 wooden staircase. The room surrounding the staircase is spacious, with large windows that allow
 2119 natural light to enter, enhancing the brightness of the space.

2120 **Human:** What is the relationship between the components, and how are they arranged?

2121 **Model:** The staircase’s design is both functional and aesthetic, with its spiral form creating a
 2122 dynamic visual element within the room. The natural light from the windows highlights the warm
 2123 tones of the wood and adds depth to the space. The absence of people or objects in the room
 2123 emphasizes the architectural features of the staircase.

2124 **Human:** Is there anything in the margins or borders of the image worth noting?

2125 **Model:** The room’s architecture is modern, with clean lines and minimalistic design elements.
 2126 The combination of the staircase’s curved form and the natural light creates an inviting and open
 2127 atmosphere in the space.

2128 **Human:** How would you describe the image in a well-organized and cohesive manner?

2129 **Model:** The image showcases a modern spiral staircase with a unique design. The staircase
 2130 features a curved, wooden handrail that is dark brown in color, contrasting with the lighter wooden
 2131 steps. The railings are made of the same dark wood and have a horizontal slat design, giving a
 2132 sense of movement along the staircase’s curve. The staircase itself appears to be constructed from
 2132 polished wood, giving it a sleek and contemporary look...

2133 Table 13: Hyperparameters, training configurations, and inference time for the SICOG implementation
 2134 in Step 4 (Section 3). Inference time is reported by data generation mode: Detailed Descriptions (D)
 2135 and Direct Answers (A) on unlabeled images from the 118k BLIP dataset, and Chain of Thought
 2136 (CoT) and CoD on unlabeled image-question pairs from the 63k LLaVA-CoT dataset.

| Model | LLaVA-Qwen2-7B | | | LLaVA-Qwen2-7B-UHD | | | LLaVA-Llama3.1-8B-UHD | | |
|--|----------------------|-----------|---------|----------------------|-----------|---------|-----------------------|-----------|---------|
| Training Stage | Stage 1 | Stage 1.5 | Stage 2 | Stage 1 | Stage 1.5 | Stage 2 | Stage 1 | Stage 1.5 | Stage 2 |
| Learning Rate | 2e-4 | 2e-5 | 2e-5 | 2e-4 | 2e-5 | 2e-5 | 2e-4 | 2e-5 | 2e-5 |
| Batch Size | 256 | 128 | 128 | 256 | 128 | 128 | 256 | 128 | 128 |
| Sequence Length | 4096 | 4096 | 4096 | 4096 | 4096 | 4096 | 4096 | 4096 | 4096 |
| Epochs | 1 | 1 | 1 | 1 | 1 | 1 | 1 | 1 | 1 |
| Training Time | 50 min | 40 min | 5.2 h | 1 h | 1.5 h | 9.5 h | 1 h | 1.8 h | 12.3 h |
| Resource (GPUs) | 4x8 NVIDIA A100 80GB | | | 4x8 NVIDIA A100 80GB | | | 4x8 NVIDIA A100 80GB | | |
| Inference Time (Self-Generating Pre-training Data) | | | | | | | | | |
| Detailed Descriptions / CoD | 4 h / 12.5 h | | | 4 h / 13 h | | | 3 h / 6.5 h | | |
| Direct Answers / CoT | 2 h / 8.5 h | | | 1.5 h / 9 h | | | 1.5 h / 9.5 h | | |
| Resource (GPUs) | 4x8 NVIDIA A100 80GB | | | 4x8 NVIDIA A100 80GB | | | 4x8 NVIDIA A100 80GB | | |

2151 • **Self-Improving Cognition (Perception & Reasoning – Ours):** Pre-training with self-generated
 2152 data, including re-caption data containing detailed descriptions (DD) and *Chain-of-Description*
 2153 (CoD), visual instruction-tuning data with direct answers (DA) and structured CoT, as well as
 2154 text-only instruction-tuning data.

2155 **M.2 IMPLEMENTATION DETAILS.**

2156 (i) *Models:* We utilize both low-resolution (LLaVA-Qwen2-7B (Liu et al., 2023)) and high-resolution
 2157 (LLaVA-Qwen2-7B-UHD (Guo et al., 2024) and LLaVA-Llama3.1-8B-UHD) models for our investi-
 2159 gation. Specifically, we employ CLIP-ViT-L/14-336 (Radford et al., 2021) as the visual encoder,

2160 Qwen2-7B-Instruct (Yang et al., 2024a) and LLaMA-3.1-8B-Instruct (Grattafiori et al., 2024) as the
 2161 backbone LLMs.

2162 (ii) *Self-Generated Data Source*: We recaption the images used for modality alignment and self-
 2163 annotate 63k image-question pairs randomly selected from LLaVA-CoT, ensuring zero overlap
 2164 with the curated training data in Section 3. Additionally, we self-annotate 100k text-only prompts
 2165 randomly sampled from OpenHermes-2.5 (Teknium, 2023).

2166 (iii) *Data Utilized in the Three-Stage Training Strategy*: During the self-refinement step (Step
 2167 4 in Figure 2), we use BLIP-558k caption data (Radford et al., 2021) for modality alignment,
 2168 following (Liu et al., 2024b). For multimodal pre-training, we use self-generated data along with
 2169 858k instruction-tuning samples organized by (Zhang et al., 2024b), which include the widely adopted
 2170 LLaVA-Mix665k (Liu et al., 2024a) and 160k samples from UReader (Ye et al., 2023).

2171 (iv) *Implementing Step 2 of SICOG*: To collect pre-training data, we prompt the model multiple times
 2172 to sample candidate outputs using a temperature of 0.7 and top-p of 0.95:

- 2174 • For image captioning, we sample three candidate captions (two in *Chain-of-Description*
 2175 format and one as a detailed description).
- 2176 • For visual instruction tuning, we sample three candidate responses (two in chain-of-thought
 2177 (CoT) format and one as a direct answer).
- 2178 • For text-only instruction tuning, we sample three candidate responses.

2179 (v) *Implementing Step 3 of SICOG*: To ensure the quality of self-generated pre-training data, we
 2180 use NV-Embed-v2 (Lee et al., 2024) to generate candidate embeddings and calculate their semantic
 2181 similarity. The data is curated based on similarity scores and predefined thresholds. Specifically, we
 2182 apply the following curation strategies:

- 2183 • **Curation of Self-Generated Image Captioning Data**: We set the similarity threshold
 $\tau^{\text{Perception}} = 0$ and retain all top-1 ranked self-generated captions in a mixture of two
 2184 formats: detailed descriptions and *Chain-of-Description*. To preserve the MLLM’s multi-
 2185 turn conversational ability, we convert the top-1 ranked *Chain-of-Description* captions with
 2186 a consistency score higher than 0.85 into a multi-turn conversational format. Detailed
 2187 examples are provided in Tables 11 and 12.

2188 In addition, Table 14 presents a comparison of two perception-enhancement approaches
 2189 for SICOG: (i) fine-tuning with 35 detailed descriptions and (ii) *Chain-of-Description* in
 2190 three formats (standard caption-only, step-by-step elicitation, and multi-turn conversation,
 2191 as shown in Tables 11 and 12). The results suggest: (1) the efficacy of the proposed *Chain-
 2192 of-Description* approach in enhancing richer visual understanding. (2) the impact of the
 2193 three different *Chain-of-Description* formats on the overall performance of SICOG.

- 2194 • **Curation of Self-Generated Visual Instruction-Tuning Data**: We set the similarity
 2195 threshold $\tau^{\text{Perception}} = 0.95$ and retain all top-1 ranked self-generated responses in two
 2196 formats: direct answers and chain-of-thought (CoT).
- 2197 • **Curation of Self-Generated Text-Only Instruction-Tuning Data**: We set the similarity
 2198 threshold $\tau^{\text{Perception}} = 0.8$ and retain only the first 50k text-only prompt-response pairs based
 2199 on their similarity score rankings.

2200 Extensive experiments and analyses are conducted using 128 A100 80G GPUs. Table 13 summarizes
 2201 the hyperparameters used to implement SICOG in Step 4 (Section 3); the same settings are also
 2202 applied in Step 1 to develop the MLLM’s capabilities during Stage 2.

2203 M.3 IMPLEMENTATION DETAILS OF COMPARED METHODS.

2204 (i) *Implementing Weak-to-Strong Distillation*: Following (Li et al., 2024a), we prompt Qwen2-VL-
 2205 72B-Instruct (Wang et al., 2024) and LLaVA-NeXT-34B (Liu et al., 2024b), two leading open-source
 2206 MLLMs known for their strong captioning capabilities, to generate high-quality captions for unlabeled
 2207 images. These captions are used as multi-modal pre-training data to construct smaller foundation
 2208 MLLMs, resulting in models such as Qwen2-VL-72B-Instruct-LLaVA-Qwen2-7B-UHD, LLaVA-
 2209 NeXT-34B-LLaVA-Qwen2-7B-UHD, and others. Generating captions for 118k unlabeled BLIP

Table 14: Comparison of two perception-enhancement approaches for SICOG: (i) fine-tuning with **35k** detailed descriptions and (ii) *Chain-of-Description* in three formats (as shown in Tables 11 and 12). Refer to Table 9 for a detailed discussion. The self-generated caption data used are sampled only once, without filtering.

| Method | Perception Enhancement | Train Data Stage 1.5 | Comprehensive | | Hallu. | Chart/Table | Knowledge | | | |
|--|------------------------|---|---------------|--------------|--------------|--------------|--------------|--------------|--------------|--------------|
| | | | MMBen. | MMStar | | | POPE | DocV. | Chart. | |
| <i>Base Model</i> | | | | | | | | | | |
| LLaVA-Qwen2-7B-UHD | - | - | 77.63 | 48.93 | 87.31 | 70.18 | 69.96 | 38.90 | 77.29 | 74.94 |
| | Fintune w/ 35k DD | Self-generated 118k caption w/ DD | 77.19 | 50.67 | 85.74 | 71.43 | 71.96 | 37.70 | 78.14 | 75.94 |
| | | Self-generated 118k caption w/ CoD (caption) | 78.25 | 50.93 | 86.80 | 71.48 | 72.12 | 40.30 | 77.84 | 76.81 |
| SICOG-LLaVA-Qwen2-7B-UHD (Perception) | Fintune w/ 35k CoD | Self-generated 118k caption w/ CoD (multi.) | 78.48 | 50.20 | 86.22 | 71.74 | 72.52 | 41.20 | 76.95 | 76.33 |
| | | Self-generated 118k caption w/ CoD (conv.) | 78.53 | 50.87 | 87.19 | 71.67 | 72.16 | 40.00 | 78.24 | 76.62 |
| | | Self-generated 118k caption w/ CoD (caption, multi., conv.) | 77.52 | 50.60 | 86.86 | 71.84 | 72.32 | 41.60 | 77.44 | 76.75 |

images using Qwen2-VL-72B-Instruct requires approximately 110 hours on a cluster of 4x8 NVIDIA A100 80GB GPUs. To facilitate reproducibility, we directly utilize the open-sourced recaptioned dataset generated by LLaVA-NeXT-34B (Liu et al., 2024b).

(ii) *Implementing Multi-Agent Collaboration*: Following (Fang et al., 2024), we employ three specialized modules—Spatial Specialist, OCR Specialist, and Grounding Specialist—to extract fine-grained attributes. These attributes are combined with self-generated detailed descriptions to form rich pre-training captions. Specifically, we prompt Qwen2-VL-72B-Instruct to generate spatial attributes using the instruction: “*Elaborate on the visual and narrative elements of the image in detail, with a focus on spatial relations.*” This annotation process, applied to the 118k unlabeled BLIP images, requires approximately 100 hours on a cluster of 4x8 NVIDIA A100 80GB GPUs. For OCR-based annotations, we utilize PaddleOCR (PaddlePaddle Team, 2020), retaining only outputs with a confidence score above 0.9. For object grounding, we adopt GroundingDINO (Liu et al., 2024c) with a detection threshold of 0.435. The OCR and grounding annotation processes take approximately 1 hour on 8 NVIDIA A100 80GB GPUs. After extracting all attributes, we use Qwen2-VL-72B-Instruct to rephrase the outputs for improved fluency and clarity. Finally, we concatenate the self-generated detailed descriptions with the spatial, OCR, and grounding attributes to construct multi-turn conversational caption data, following the methodology of (Fang et al., 2024).

2268 **N ANALYSIS OF COMPUTATIONAL COST**
22692270 Table 15: Computational analysis of the compared pre-training approaches for generating the pre-
2271 training data.
2272

| 2273 Method | 2274 Generation Task | 2275 Model(s) Used | 2276 Hardware (A100 80G) | 2277 Time (Hours) | 2278 Est. GPU-Hours (Total) |
|---|---|---------------------------|---------------------------------|--------------------------|------------------------------------|
| <i>External Model Distillation</i> | | | | | |
| 2277 Strong-to-Weak 2278 Distillation | Detailed Descriptions | Qwen2-VL-72B-Instruct | 32 GPUs | ~110 | ~3,520 |
| 2279 Multi-Agent 2280 Collaboration | Spatial Attributes | Qwen2-VL-72B-Instruct | 32 GPUs | ~100 | ~3,200 |
| | OCR Annotation | PaddleOCR | 8 GPUs | ~1 | ~8 |
| | Grounding Information | GroundingDINO | 8 GPUs | ~1 | ~8 |
| | Detailed Descriptions | Qwen2-VL-72B-Instruct | 32 GPUs | ~115 | ~3,680 |
| <i>Self-Improving (Ours)</i> | | | | | |
| 2285 <i>SICOG</i> | Post-Training Optimization | LLaVA-Qwen2-7B-UHD | 32 GPUs | ~2 | ~64 |
| | Detailed Captions (DD & CoD) | LLaVA-Qwen2-7B-UHD | 32 GPUs | ~21 | ~672 |
| | VQA Responses (DA & CoT) | LLaVA-Qwen2-7B-UHD | 32 GPUs | ~12 | ~384 |
| | Text-Only Responses | Qwen2-7B-Instruct | 8 GPUs | ~8 | ~64 |
| | Candidate Filtering (Captions, VQA, Text-only) | NV-Embed-v2 | 8 GPUs | ~20 | ~160 |
| | | | | | |

2292 The core difference between pre-training approaches lies in how multimodal pre-training data is
2293 obtained. Table 15 presents a computational cost analysis of the compared approaches for generating
2294 multimodal pre-training data. While SICOG involves more training stages compared to prevalent
2295 approaches that rely on external advanced or expert models, it significantly reduces computational
2296 cost in terms of GPU hours.

2297 We would also like to emphasize that SICOG is not designed to directly compete with existing
2298 pre-training methods that depend on external annotations. Instead, it is tailored for scenarios where
2299 high-quality external annotations are unavailable—such as when model capabilities surpass human
2300 performance, when obtaining annotations is prohibitively expensive, or when no stronger model
2301 exists to provide annotations. Additionally, SICOG can complement methods that leverage external
2302 annotations when such resources are accessible.

2322 **O MITIGATING POTENTIAL PERFORMANCE SATURATION AND ERROR**
 2323 **PROPAGATION**

2325 Table 16: Exploration of Mitigating Potential Performance Saturation

| 2328 Method | 2329 Comprehensive | | 2330 Hallu. | | 2331 Chart/Table | | 2332 Knowledge | |
|--------------------------------------|---------------------------|--------------------|--------------------|-------------------|-------------------------|-------------------|-----------------------|------------------|
| | 2330 MMBen. | 2331 MMStar | 2331 POPE | 2332 DocV. | 2332 Chart. | 2333 Math. | 2334 Science. | 2335 AI2D |
| 2330 LLaVA-Qwen2-7B-UHD | 77.63 | 48.93 | 87.31 | 70.18 | 69.96 | 38.90 | 77.29 | 74.94 |
| 2331 Self-Caption-LLaVA-Qwen2-7B-UHD | 77.41 | 49.30 | 86.67 | 70.16 | 71.32 | 38.90 | 76.40 | 75.87 |
| 2332 SICOG-LLaVA-Qwen2-7B-UHD | 78.08 | 52.47 | 87.84 | 73.70 | 73.12 | 41.40 | 79.42 | 78.40 |

2334 Table 17: Exploration of Mitigating Error Propagation

| 2336 Method | 2337 Comprehensive | | 2338 Hallu. | | 2339 Chart/Table | | 2340 Knowledge | |
|---|---------------------------|--------------------|--------------------|-------------------|-------------------------|-------------------|-----------------------|------------------|
| | 2337 MMBen. | 2338 MMStar | 2338 POPE | 2339 DocV. | 2339 Chart. | 2340 Math. | 2341 Science. | 2342 AI2D |
| 2338 LLaVA-Qwen2-7B-UHD | 77.63 | 48.93 | 87.31 | 70.18 | 69.96 | 38.90 | 77.29 | 74.94 |
| 2339 SICOG-LLaVA-Qwen2-7B-UHD w/o Filtering | 77.97 | 50.87 | 87.56 | 72.97 | 73.64 | 39.50 | 77.84 | 76.98 |
| 2340 SICOG-LLaVA-Qwen2-7B-UHD | 78.08 | 52.47 | 87.84 | 73.70 | 73.12 | 41.40 | 79.42 | 78.40 |

2342 To mitigate the potential risks of relying on the model to generate its own data, particularly in terms
 2343 of performance saturation and error propagation. To mitigate these risks, we have implemented the
 2344 following measures:

2345 *Mitigating Performance Saturation.* Our framework enhances the model’s perception and reasoning
 2346 abilities using minimal annotations during Stage 1. By ensuring meaningful improvements in the base
 2347 model before initiating self-improvement iterations, we establish a robust self-improving paradigm.
 2348 Below, we provide results leveraging the model’s self-generated detailed captions as pre-training
 2349 data (since the base model cannot generate chain-of-thought reasoning). This variant is referred to as
 2350 “Self-Caption-LLaVA-Qwen2-7B-UHD.” In Table 16, we observe that SICOG-LLaVA-Qwen2-7B-
 2351 UHD achieves superior performance, highlighting the value of fine-tuning with minimal annotated
 2352 data during Stage 1 to ensure performance improvements.

2353 *Avoiding Error Propagation.* We employ a robust data filtering mechanism to select high-quality
 2354 self-generated data for pre-training, as detailed in Section 3. This minimizes the impact of noisy
 2355 or biased outputs. Below, we present results after removing the filtering mechanism (denoted as
 2356 “w/o Filtering”). In Table 17, SICOG-LLaVA-Qwen2-7B-UHD demonstrates improved performance
 2357 when the filtering mechanism is applied, underscoring its importance in enhancing the self-improving
 2358 paradigm.

2359 While these measures address the immediate risks, we acknowledge the importance of further
 2360 refinement. We aim for SICOG to serve as a starting point for advancing self-improvement techniques
 2361 and are committed to exploring additional strategies to ensure robustness in future iterations.

2362
 2363
 2364
 2365
 2366
 2367
 2368
 2369
 2370
 2371
 2372
 2373
 2374
 2375

P ADDITIONAL EXPERIMENTAL RESULTS

Table 18: Additional evaluation results on MMMLU-Val (Yue et al., 2024a).

| Method | Type | MMMLU |
|--|-----------------------------|--------------|
| LLaVA-Qwen2-7B-UHD | - | 55.38 |
| Qwen2-VL-72B-Instruct-LLaVA-Qwen2-7B-UHD | Strong-to-Weak Distillation | 52.25 |
| Multi-Experts-LLaVA-Qwen2-7B-UHD | Multi-Experts | 52.25 |
| SICOG-LLaVA-Qwen2-7B-UHD | Self-Learning | 56.88 |

Table 19: Comparison with other pre-training methods.

| Method | Comprehensive | | Hallu. | Chart/Table | Knowledge | | | |
|---------------------------------------|---------------|--------------|--------------|--------------|--------------|--------------|--------------|--------------|
| | MMBen. | MMStar | | | POPE | DocV. | Chart. | Math. |
| LLaVA-Qwen2-7B-UHD | 77.63 | 48.93 | 87.31 | 70.18 | 69.96 | 38.90 | 77.29 | 74.94 |
| Self-Caption- | 77.41 | 49.30 | 86.67 | 70.16 | 71.32 | 38.90 | 76.40 | 75.87 |
| LLaVA-NeXT-34B-Caption- | 77.75 | 50.60 | 86.46 | 71.20 | 71.56 | 36.90 | 78.38 | 76.00 |
| LLaVA-NeXT-34B-Caption-GPT-4o-Reason- | 77.80 | 51.27 | 87.00 | 72.20 | 72.80 | 37.80 | 78.93 | 77.49 |
| SICOG-LLaVA-Qwen2-7B-UHD | 78.08 | 52.47 | 87.84 | 73.70 | 73.12 | 41.40 | 79.42 | 78.40 |

Results on MMMLU. Due to space limitations, we present the results on the MMMLU-Val dataset in Table 18.

Comparison with other pre-training methods. Existing open-source models lack the ability for systematic perception and reasoning. Specifically, directly prompting these models to generate Chain-of-Description (CoD) captions and structured Chain-of-Thought (CoT) reasoning data (Xu et al., 2025) is impractical. Furthermore, none of the backbone models used in this work possess multimodal CoT reasoning abilities, as their training data does not include multimodal CoT reasoning examples. This provides a clear framework to evaluate how incorporating self-generated CoT data during pre-training impacts model performance.

We also provide additional results in Table 19:

1. *Comparison with pre-training using re-captioned data generated via prompting the base model (Self-Caption-LLaVA-Qwen2-7B-UHD).*

2. *Comparison with pre-training using re-captioned data from a stronger captioning model and CoT reasoning data.* Specifically, we use LLaVA-NeXT-34B for captioning and GPT-4o for CoT reasoning data, curated in Xu et al. (2025) (LLaVA-NeXT-34B-Caption-GPT-4o-Reason-LLaVA-Qwen2-7B-UHD).

Our approach, SICOG-LLaVA-LLaVA-Qwen2-7B-UHD, outperforms these methods, demonstrating the effectiveness of incorporating self-generated CoT data during pre-training.

2430 **Q PROMPTS**

2431

2432

2433 Table 20: The prompt utilized by GPT-4o for eliciting *Chain-of-Description* for image-captioning
2434 training datasets.

2435 **Prompt Used by GPT-4o for eliciting *Chain-of-Description***

2436

2437 You are an expert AI assistant tasked with analyzing an image and generating a detailed, step-by-step
2438 description. You are provided with an original description as a reference. Your goal is to ensure accuracy,
2439 clarity, and logical progression in your response. Follow these guidelines:

2440 **Guidelines:**

2441

1. **Ensure Comprehensive Coverage:** Identify and include all relevant details visible in the image. Avoid unnecessary repetition or irrelevant information.
2. **Avoid Adding Imaginary Details:** Base your reasoning strictly on what is visible in the image or provided in the description. Do not include fabricated or unverifiable details.
3. **Incorporate Relevant Context:** Add factual, relevant context to enhance understanding where appropriate, but ensure it aligns strictly with the visible or provided content.
4. **Prevent Inaccuracies:** Stick to the given data. Avoid assumptions or deviations from the available evidence.

2447 **Step-by-Step Process:**

2448 **Step 1: Extract salient content by identifying the key elements that define the image.**

2449 *Example:* The image is a monochrome photocopy of a document that appears to be a page of meeting or
2450 project notes. It contains both typed and handwritten text, with a focus on tasks and progress updates related
2451 to paper-related issues. The document includes a reference number at the bottom and a source URL.

2452 **Step 2: Analyze detailed information, focusing on instance-level attributes such as low-level and
2453 fine-grained details.**

2454 *Example:* The document lists several tasks, such as checking with "KC" on the possibility of putting bands
2455 "long-ways," which is marked as "In progress." Other tasks include checking on "shrinking" paper, which is
2456 also "In progress," and checking the commercial viability of banded papers, marked as "Okay." There are
2457 handwritten notes and checks next to some points, indicating their status.

2458 **Step 3: Consider relational-level attributes, analyzing interactions between elements and their spatial
2459 organization.**

2460 *Example:* The tasks are organized in a list format, with some items having associated handwritten notes that
2461 indicate completion or ongoing status. The name "Jimmy Wu" is associated with an action item regarding
2462 a DC work request with KC banded papers, awaiting approval for banded additives. The document also
2463 mentions running "GPC KS and KOOL KS on RIP-4 (LCC)" and notes that KC is running "cross-hatch"
2464 papers.

2465 **Step 4: Examine marginal or peripheral content to ensure no important information is missed.**

2466 *Example:* The document specifies that the next meeting is scheduled for Monday, February 7, at 9:00 a.m. in
2467 the International Conference Room. The reference number "584100571" is located at the bottom of the page,
2468 and the source URL is included at the bottom.

2469 **Step 5: Organize all observations into a detailed, cohesive description.**

2470 *Example:* The image is a monochrome photocopy of a document that appears to be a page of meeting or
2471 project notes, containing both typed and handwritten text. The document lists several tasks related to paper-
2472 related issues, such as checking with "KC" on the possibility of putting bands "long-ways," which is marked
2473 as "In progress," and checking the commercial viability of banded papers, marked as "Okay." Handwritten
2474 notes and checks next to some points indicate their status. The name "Jimmy Wu" is associated with an
2475 action item regarding a DC work request with KC banded papers, awaiting approval for banded additives.
2476 Other items include running "GPC KS and KOOL KS on RIP-4 (LCC)" and KC running "cross-hatch"
2477 papers. The next meeting is scheduled for Monday, February 7, at 9:00 a.m. in the International Conference
2478 Room. The document is marked with a reference number "584100571" at the bottom, and a source URL is
2479 included.

2480 **Important Notes:**

2481 - **Steps 1–4**: Write concise observations in one or two sentences each.

2482 - **Step 5**: Summarize all observations into a detailed paragraph or two, as descriptive as necessary.

2483 **Input:** <image>| Question: Could you please transcribe the image into a descriptive paragraph? Explain
2484 your description step-by-step. Original description: <caption>

2485 **Output:**

2484

2485

2486

2487

2488

2489

Table 21: The prompt utilized by GPT-4o for evaluating the quality of re-captioned data.

2490

2491

Prompt Used by GPT-4o to Evaluate Image Caption Quality

2492

2493

2494

2495

2496

Evaluation Process:

2497

2498

1. **Critique First:** Begin by generating a concise critique of the caption. Highlight both its strengths and weaknesses in plain language. Focus on how well the caption describes the image and aligns with the criteria.

2499

2500

2. **Score Each Criterion:** After the critique, provide a score for each evaluation criterion on a scale from 1 to 5. Ensure the scores are consistent with the critique and avoid contradictions.

2501

2502

Evaluation Criteria:

Evaluate the caption based on the following eight dimensions:

2503

2504

1. **Salient Content:** Does the caption highlight the key elements and most important details of the image?

2505

2506

2. **Fine-Grained Details:** Does the caption include specific attributes, such as textures, colors, or text found in the image?

2507

2508

3. **Relational Attributes:** Does the caption describe interactions or spatial relationships between elements in the image?

2509

2510

4. **Peripheral Content:** Does the caption include additional relevant details that enhance completeness without being redundant?

2511

2512

5. **Faithfulness:** Does the caption accurately describe what is visible in the image without adding imaginary or false information?

2513

6. **World Knowledge:** Does the caption incorporate relevant world knowledge, such as context or implied meaning, to enhance its coherence?

2514

Scoring Rubric:

2515

- **Poor (1):** Fails to meet the criterion.

2516

- **Fair (2):** Partially meets the criterion but has noticeable shortcomings.

2517

- **Average (3):** Adequately meets the criterion but lacks depth or sophistication.

2518

- **Good (4):** Strongly aligns with the criterion and demonstrates nuanced understanding.

- **Excellent (5):** Perfectly aligns with the criterion with high-quality descriptions.

2519

Output Format: Follow this structured format exactly:

2520

1. **Critique:** Write a concise critique (2-4 sentences), summarizing the strengths and weaknesses.

2521

2. **Scores:** Provide a score for each dimension using the following format:

2522

- Salient Content: Score = [[Your Score]]

2523

- Fine-Grained Details: Score = [[Your Score]]

2524

- Relational Attributes: Score = [[Your Score]]

2525

- Peripheral Content: Score = [[Your Score]]

2526

- Faithfulness: Score = [[Your Score]]

2527

- World Knowledge: Score = [[Your Score]]

Important Notes:

2528

- Focus solely on the caption's alignment with the criteria and the image content.

2529

- Be objective, impartial, and avoid introducing biases.

2530

- Do not let the caption's length, style, or structure influence your evaluation unless it directly affects quality.

2531

- Ensure your response is clear, concise, and follows the exact output format.

2532

Input: |<image>| Caption: |<caption>|

2533

Output:

2534

2535

2536

2537

2538 **R TRAINING EXAMPLES**

2539

2540 Table 22: An example from the image captioning training dataset curated to elicit systematic
 2541 multimodal perception.

2543 **Image Captioning Data for Enhancing Systematic Multimodal Perception**

2544



2554 **Example with Detailed Description Caption Format**

2555 **Prompt:**

2556 Please provide a vivid description of the image.

2557 **Caption:**

2558 The image features a person with long, red hair sitting cross-legged on a bed, playing an acoustic guitar. They
 2559 are wearing a dark blue shirt with rolled-up sleeves and black pants, appearing focused on the instrument. The
 2560 guitar is a classic wooden brown with light-colored frets. In front of them, an open laptop on a small table
 2561 or stand suggests they might be following music or a tutorial. The room exudes a warm ambiance with soft
 2562 lighting, and the colorful bedspread adds vibrancy. Decorations like string lights and wall hangings contribute to
 2563 a bohemian aesthetic, while a dresser with various personal items in the background adds a personal touch to the
 2564 space.

2565 **Example with our proposed *Chain-of-Description* Caption Format**

2566 **Prompt:**

2567 Please provide a vivid description of the image. Describe the image step-by-step.

2568 **Caption:**

2569 **Step 1: Extract salient content by identifying the key elements that define the image.**

2570 The image depicts a person with long, red hair sitting cross-legged on a bed, playing an acoustic guitar. The
 2571 person is dressed in a dark blue shirt with rolled-up sleeves and black pants. An open laptop is positioned on a
 2572 small table or stand in front of them, suggesting they might be using it for guidance, such as following music
 2573 sheets or a tutorial.

2574 **Step 2: Analyze detailed information, focusing on instance-level attributes such as low-level and fine-
 2575 grained details.**

2576 The guitar is a classic wooden brown with light-colored frets. The room has a warm ambiance, enhanced by soft
 2577 lighting. The bedspread is colorful, adding vibrancy to the scene. Decorations such as string lights and wall
 2578 hangings contribute to a bohemian aesthetic. In the background, there is a dresser with various personal items,
 2579 adding to the lived-in feel of the space.

2580 **Step 3: Consider relational-level attributes, analyzing interactions between elements and their spatial
 2581 organization.**

2582 The person is seated on the bed, with the guitar resting on their lap, indicating engagement with the instrument.
 2583 The laptop's placement suggests it is being actively used, possibly for learning or playing along with music. The
 2584 string lights and wall hangings are positioned to create a cozy and artistic environment.

2585 **Step 4: Examine marginal or peripheral content to ensure no important information is missed.**

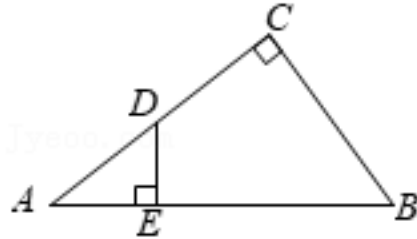
2586 The room's decor, including the string lights and wall hangings, adds a personal touch and suggests a creative or
 2587 artistic personality. The dresser in the background, with its assortment of items, further personalizes the space.

2588 **Step 5: Organize all observations into a detailed, cohesive description.**

2589 The image features a person with long, red hair sitting cross-legged on a bed, playing an acoustic guitar. They
 2590 are wearing a dark blue shirt with rolled-up sleeves and black pants, appearing focused on the instrument. The
 2591 guitar is a classic wooden brown with light-colored frets. In front of them, an open laptop on a small table
 2592 or stand suggests they might be following music or a tutorial. The room exudes a warm ambiance with soft
 2593 lighting, and the colorful bedspread adds vibrancy. Decorations like string lights and wall hangings contribute to
 2594 a bohemian aesthetic, while a dresser with various personal items in the background adds a personal touch to the
 2595 space.

2592
2593
2594
2595
2596
2597

Table 23: An example from the visual instruction-following training dataset designed to enhance systematic multimodal reasoning.

2598
2599
2600**Visual Instruction-Following Data for Enhancing Systematic Multimodal Reasoning****Example 1: Open-Ended Problem**2601
2602
2603
2604
2605
2606
2607
2608
2609
2610
2611
2612
2613
2614**Example with Direct Answer Response Format****Question:**

In the right triangle ABC , $\angle C = 90^\circ$, point D is a point on AC , $DE \perp AB$ at point E , $AB = 10$, $BC = 6$, $DE = 2.4$, then the length of AD is ()

A. 1.2 B. 3 C. 4 D. 5

Response:

C

2615
2616
2617
2618
2619
2620
2621
2622
2623
2624
2625
2626
2627**Example with Chain-of-Thought Response Format****Question:**

In the right triangle ABC , $\angle C = 90^\circ$, point D is a point on AC , $DE \perp AB$ at point E , $AB = 10$, $BC = 6$, $DE = 2.4$, then the length of AD is ()

A. 1.2 B. 3 C. 4 D. 5

Answer the question step by step.

Response:**Step 1: Clarify the task objective.**

To solve this problem, I will use the properties of similar triangles and the known measurements provided. By identifying similar triangles, I can set up a proportion to find the length of AD .

Step 2: Extract the crucial visual information from the image.

The image shows right triangle ABC with $\angle C = 90^\circ$. Point D is on segment AC , and DE is perpendicular to AB at point E . Measurements are given as $AB = 10$, $BC = 6$, and $DE = 2.4$.

Step 3: Generate detailed reasoning to solve the task.

In the right triangle ABC , $\angle C = 90^\circ$. DE is perpendicular to AB , making $\angle AED$ also equal to 90° . Because both triangles ADE and ABC share angle A , triangle ADE is similar to triangle ABC by AA similarity (Angle-Angle). Using the similarity of triangles ADE and ABC , we can set up the proportion:

$$\frac{AD}{DE} = \frac{AB}{BC}$$

Substituting the known values:

$$\frac{AD}{2.4} = \frac{10}{6}$$

Simplifying the right side:

$$\frac{10}{6} = \frac{5}{3}$$

Thus, the proportion becomes:

$$\frac{AD}{2.4} = \frac{5}{3}$$

Solving for AD :

$$AD = \frac{5}{3} \times 2.4 = 4$$

Step 4: Conclude the task with an answer.

C

2643
2644
2645

2646
2647
2648
2649
2650
2651
2652
2653

2654 Table 24: An example from the visual instruction-following training dataset designed to enhance
2655 systematic multimodal reasoning.

2656
2657
2658
2659
2660
2661
2662
2663
2664
2665
2666
2667
2668
2669

Visual Instruction-Following Data for Enhancing Systematic Multimodal Reasoning

Example 2: Multiple-Choice Problem



Example with Direct Answer Response Format

Question:

Why is the person in the air?

A. Grabbing a frisbee B. Falling C. Angry D. Bouncing

Response:

A

Example with Chain-of-Thought Response Format

Question:

Why is he in the air?

A. grab frisbee B. falling C. angry D. bouncing

Answer the question step by step.

Response:

Step 1: Clarify the task objective.

I will analyze the image to determine why the person is in the air by examining relevant visual clues. I'll then follow a reasoning process to arrive at the correct answer.

Step 2: Extract the crucial visual information from the image.

The image shows an indoor sports setting with a person in mid-air holding an object that resembles a frisbee. The individual is wearing athletic gear, and there is a goal visible in the background, suggesting a sports activity.

Step 3: Generate detailed reasoning to solve the task.

Considering the context and the object in hand, it appears the person is actively participating in a sport involving a frisbee. The position of the person suggests they might be jumping to grab or throw the frisbee. The presence of a goal could imply that the activity requires throwing the frisbee accurately, which aligns with the action of jumping.

Step 4: Conclude the task with an answer.

A

2692
2693
2694
2695
2696
2697
2698
2699

2700 S LIMITATIONS 2701

2702 While our experimental results are promising, we consider these findings preliminary, as many aspects
2703 of this field remain unexplored.
2704

2705 **Dealing with Trade-Offs between Structured and Unstructured Data.** We currently adopt two
2706 structured methodologies to elicit high-quality multimodal data. While effective, these approaches
2707 may serve as a “temporary shortcut” for enhancing model capabilities (Wei & Chung, 2024). To
2708 encourage “describing or (implicit) thinking freely,” we also incorporate a mix of detailed descrip-
2709 tions and direct answers. Future work may further explore the trade-offs between structured and
2710 unstructured data.
2711

2712 **Balancing Data Ratios and Formats in Self-Generated Pre-Training Data.** Our study primarily
2713 aims to establish a starting point for building next-generation foundation MLLMs through a fully
2714 self-improving paradigm. As such, we did not focus on optimizing the balance of data types or
2715 formats within the self-generated pre-training corpus. Nevertheless, Appendix G shows that varying
2716 the proportions of caption data, visual instruction tuning data, and text-only prompts significantly
2717 impacts SICOG’s performance. Furthermore, Table 14 demonstrates that even when using the same
2718 CoD data, different formatting yields different results. Future work may investigate how balancing
2719 data ratios and formats can further optimize self-improvement.
2720

2721 **Leveraging More Advanced Quality Evaluation Methods.** We employ a simple but effective
2722 self-consistency mechanism to select high-quality outputs for unlabeled images, image–question pairs,
2723 and text-only prompts, based on semantic coherence. Future work may benefit from incorporating
2724 more advanced quality evaluation methods to further enhance data selection.
2725
2726
2727
2728
2729
2730
2731
2732
2733
2734
2735
2736
2737
2738
2739
2740
2741
2742
2743
2744
2745
2746
2747
2748
2749
2750
2751
2752
2753